ÉCOLE POLYTECHNIQUE
FÉDÉRALE DE LAUSANNE

CHOICE OF RECORDED ACCELERATION TIME HISTORIES FOR NON-LINEAR SEISMIC ANALYSIS OF REINFORCED CONCRETE STRUCTURES

RESEARCH PROJECT REPORT

Philippe Schwab, Pierino Lestuzzi
IS-IMAC

Martin Koller, Corinne Lacave
RÉSONANCE Ingénieurs-Conseils SA

Publication N° 2
AUGUST 2003

APPLIED COMPUTING AND MECHANICS LABORATORY

CIVIL ENGINEERING SECTION

SCHOOL OF ARCHITECTURE, CIVIL AND ENVIRONMENTAL ENGINEERING

Abstract

The research project presented here dealt with an important aspect of seismic structural response that is still not fully understood. Its objective was to develop criteria to choose suitable earthquake recordings (acceleration time histories) to be used in non-linear dynamic analyses for seismic design, evaluation and upgrade of ductile reinforced concrete structures.

If several earthquake recordings have the same spectral acceleration at the natural frequency of a single-degree-of-freedom-system (SDOF system), the same displacement demand would result for this SDOF system from linear response spectra analyses. However, non-linear dynamic analyses would lead to different displacement or ductility demands. The key question is what characteristics of the earthquake recordings influence the system's displacement or ductility demand. The structural engineer will only be in a position to choose the earthquake recordings for non-linear dynamic analyses in a rational manner once this question is answered.

The methodology of the present study consisted of systematic investigations of the non-linear response of SDOF systems subjected to different earthquake recordings. The structural behaviour is described by six different recognised hysteretic models. 164 earthquake recordings, taken from the European Strong Motion Database, were used in this study.

The final displacement or ductility demand of the SDOF systems was correlated with different earthquake characteristics, such as effective peak ground acceleration, spectral acceleration, slope of response spectra, spectral intensity, etc. As expected from the literature, the spectral intensity defined by Nau and Hall gives a fairly good correlation with the displacement or ductility demand. A modified spectral intensity is proposed here in order to improve this correlation. This modification takes into account the structure's "initial" natural frequency and the design ductility. As a conclusion, recommendations for structural engineers are formulated that are believed to increase the reliability of non-linear seismic analyses.

In addition, the impact of "fling" on structural behaviour was addressed, too. Fling is a strong velocity pulse that results in permanent ground displacement. It has been observed in recent earthquake recordings stemming from stations situated close to the earthquake source. 18 recordings of the Chi-Chi Taiwan (1999) earthquake containing fling were applied to the SDOF systems. The resulting ductility demand was compared with the one of the same recordings after extraction of the fling. In many cases, the results obtained showed relatively small differences. Surprisingly, where differences occurred, larger displacement or ductility demands resulted for the recordings without fling, with the exception of one single case. The reasons for this peculiar result are not yet understood. It can be concluded that much more research work is needed in order to understand the impact of fling on engineering structures.

Table of content

1. Introduction

The research project presented here dealt with an important aspect of seismic structural response that is still not fully understood. Its objective was to develop criteria to choose suitable earthquake recordings to be used in non-linear dynamic analyses for seismic design, control and upgrade of reinforced concrete (RC) structures.

Standard simplified methods of seismic calculation generally contain an unknown margin of conservatism. This is usually a minor problem for new structures, the cost of an unnecessary conservative margin being most of the time insignificant. The situation, however, is different for existing structures: A conservative recalculation may lead to the result that the structure is unsafe, whereas a more realistic calculation would show that it is safe enough. Money may be spent unnecessarily for upgrading. Since one "unit of earthquake safety" is more expensive to be obtained for an existing building than for a new one, it is important to predict the seismic behaviour of existing structures as realistically as possible. Non-linear dynamic time history analyses are usually thought to be the most realistic approach.

Up to now, if non-linear dynamic analyses were performed, they were usually done with artificial acceleration time histories. The reason is that until recently, there were not enough recordings of acceleration time histories available. Furthermore, most engineers believe that artificial time histories covering the whole frequency range of a design response spectrum represent a conservative input for the analysis. However, this is not necessarily true for non-linear systems. Since more and more recorded time histories have become available in recent times, it would now often be possible to work with recorded time histories. However, no aid is given to the engineer how to choose time histories that are appropriate to a given design or upgrade situation.

If several acceleration time histories have the same spectral acceleration at the natural frequency of a single-degree-of-freedom-system (SDOF system), the same displacement or ductility demand would result for this SDOF system from standard response spectra analyses. However, non-linear dynamic analyses would lead to different displacement or ductility demands. The key question is what characteristics of the acceleration time history influence the system's displacement or ductility demand. The structural engineer will only be in a position to choose the earthquake recordings for non-linear dynamic analyses in a rational manner once this question is answered.

The research project presented here aimed at answering that question. As a conclusion, recommendations for structural engineers are formulated that are believed to increase the reliability of non-linear seismic analysis.

The final part of this research project was devoted to a recent open question in engineering seismology and earthquake engineering: the impact of "fling" on structural behaviour. Fling is a strong velocity pulse that results in permanent ground displacement. It has been observed in recent earthquake recordings stemming from stations situated close to the earthquake source. The displacement and ductility demands were calculated for time histories containing fling before and after extracting the fling, and the results were compared with each other. In order to guide their future research, the seismologists would like to know from the engineers whether fling significantly influences structural behaviour or not.

2. Methodology

2.1 Structures

In the current study, it was chosen to model RC structures by means of non-linear SDOF systems and use their displacement and ductility demands as the decisive characteristics of the non-linear response. Each SDOF system is defined by its:

- "initial" natural frequency (f_0 = 0.25; 0.5; 0.75; 1.0; 1.5; 2.0; 3.0 and 4.0 Hz)
- yield displacement (d_y)
- hysteretic model (six recognized hysteretic models)

The initial natural frequency corresponds to the mean stiffness between the position at rest and the position at first yielding of the structure.

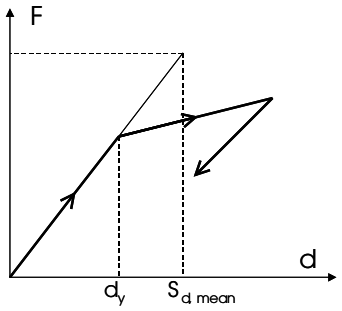

Figure 1: Definition of the structure.

For a given natural frequency, the yield displacement is chosen as being (Fig. 1):

$$d_y = \frac{S_{d,mean}}{R}$$

where $S_{d,mean}$ represents the mean value of the spectral displacements of the recorded time histories that were used. R is the strength reduction factor that takes the following values: 2, 3, 4 and 5. This means that for a given initial natural frequency and a given strength reduction factor, an identical SDOF system is subjected to the different acceleration time histories. Therefore, for the consideration of the correlation coefficients, displacement and ductility demand are interchangeable. They are related by the yield displacement d_y, being the same for all time histories. Therefore, the results and conclusions are valid for displacement as well as for ductility demand.

The six hysteretic models that were considered are illustrated and described in appendix A.1. The displacement and ductility demands were computed for each of the six hysteretic models. As they all yielded very similar results, it was decided to only focus on the Takeda model for the interpretation of the results.

2.2 Earthquake recordings

2.2.1 Database

A database of 164 recorded time histories was extracted from the European Strong Motion Database (Smit et al., 2000). Only time histories with a peak horizontal acceleration (PHA) of at least 0.6 m/s^2 were used, 0.6 m/s^2 being the peak ground acceleration of zone 1 in the Swiss building code SIA 261. Furthermore, only recordings for magnitude values of at least M = 5.0 were maintained in the data

base (no distinction was made for different definitions of magnitude), since lower magnitude events rarely cause structural damage. No condition was imposed on epicentral distance while selecting the time histories. Figure 2 shows the distribution of the magnitude with respect to the epicentral distance.

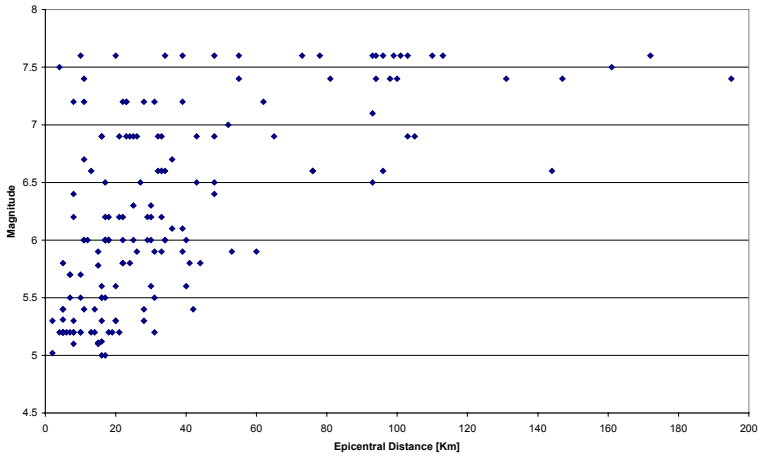

Figure 2: Magnitude versus epicentral distance plot for the 164 events.

2.2.2 Earthquake characteristics

A literature review led to the selection of earthquake characteristics as described below.

The **peak horizontal acceleration**, also called peak ground acceleration (PGA) (Elenas, 2002), which is known to correlate badly with structural response, was chosen here for reference.

PGA is sometimes a bad indicator as an acceleration time history might have a sudden peak in an otherwise low energy ground motion. Hence, a further parameter called **effective peak ground acceleration** (EPGA) is used according to Musson (2002). EPGA is defined as the mean of the spectral acceleration between 0.1 s and 0.5 s at an interval of 0.02 s, divided by a standard spectral amplification of 2.5.

The **magnitude** is also examined. The values used are those given in the European Strong Motion Database (Smit et al., 2000). They may correspond either to the moment magnitude M_W, the surface wave magnitude M_S or the local M_L magnitude.

The **Arias intensity duration** is the interval during which a certain proportion of the total Arias intensity gets accumulated. The definition used by Elenas (2002) is chosen here.

The **uniform duration**, originally proposed by Bolt using narrow band filtered accelerograms, is the sum of the intervals during which the absolute acceleration level exceeds a particular threshold (Bommer et al, 1999), here 0.5 m/s^2.

The **spectral acceleration (S_a)** is the best-known parameter to structural engineers. It is the peak elastic acceleration of a SDOF system for the entire range of frequencies or periods for a given damping ratio, here being 5%.

The **spectral intensity** is based on the pseudo-velocity response spectrum. The definition given by Nau et Hall (1984) is called **SI a** in the current study:

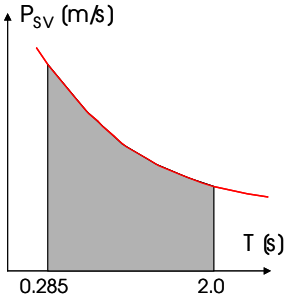

$$SI\ a(\zeta) = \frac{1}{1.715}\int_{0.285}^{2.0} P_{SV}(\zeta)\cdot dT\ , \qquad \zeta = 5\%$$

A new definition of **spectral intensity**, called **SI b** in the current study, is introduced. The interval used for the computation is closely related to the expected structural seismic response.

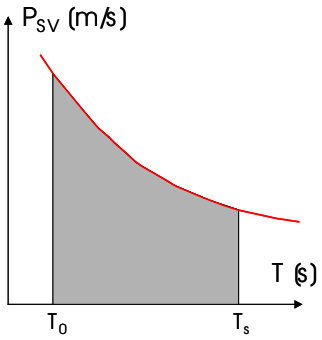

$$SI\ b(\zeta, f_0, R) = \frac{1}{\Delta T}\int_{T_0}^{T_s} P_{SV}(\zeta)\cdot dT\ , \quad \zeta = 5\%\ ,$$

$$T_s = T_0 \cdot \sqrt{R} = \frac{\sqrt{R}}{f_0}$$

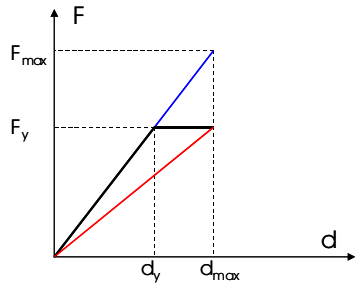

The period T_s corresponds to the secant stiffness that can easily be linked to the initial fundamental period T_0 if the equal displacement rule is assumed. The slope of the steep line in the figure beside corresponds to the initial fundamental period T_0. The slope of the less inclined line corresponds to the secant period T_s.

Since the initial fundamental vibration characteristics of RC elements change due to the occurrence of damage, it makes sense to analyse the **slope m** of the acceleration response spectrum (S_a) between the initial (f_0) and the degraded (f_s) natural frequency.

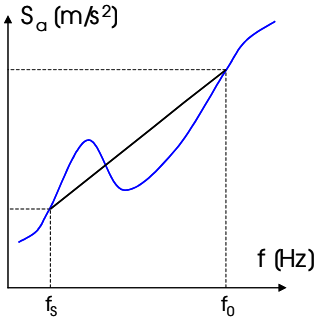

$$m(\zeta, f_0, R) = \frac{S_a(f_0,\zeta) - S_a(f_s,\zeta)}{f_0 - f_s}\ ,$$

with

$$\zeta = 10\% - 20\% - 30\%\ ,$$

$$f_s = \frac{f_0}{\sqrt{R}}$$

The major drawback of the slope characteristic is that it has to be performed in a highly damped response spectrum. It was therefore decided to smooth the jagged spectrum by using the **average slope $\overline{m}$** related to a 5 % damped response spectrum as usual.

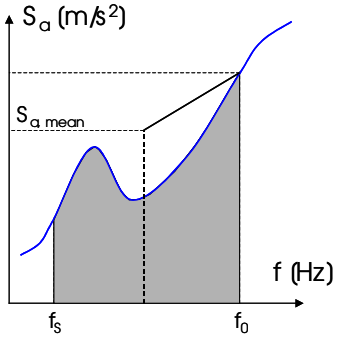

$$\overline{m}(\zeta, f_0, R) = \frac{S_a(f_0,\zeta) - S_{a,mean}(f_0,\zeta)}{\frac{f_0 - f_s}{2}}, \quad \zeta = 5\%,$$

$$S_{a,mean}(f_0,\zeta) = \frac{\int_{f_s}^{f_0} s_a(\zeta)\cdot df}{f_0 - f_s}$$

2.3 Computation of correlation coefficients

For the various SDOF models, defined by f_0 and R, the correlation coefficients between the displacement or ductility demand and the examined earthquake characteristics were computed. The details of the results are presented in graphs as a function of the initial fundamental frequency in the appendices A.2 to A.7. Correlation coefficients superior to 0.6 were considered as significant. An example of a poor and a good correlation is given in Figures 4 and 6, respectively.

3. Resulting correlation coefficients

The direct use of the original acceleration time histories for the computation of the correlation coefficients would lead to some difficulties in interpreting the results because of the large scatter of the recorded spectral accelerations (see appendix A.2). The original acceleration time histories were therefore scaled in such a way that they all had the same spectral acceleration at the SDOF system's initial natural frequency, namely the mean value $S_{a,mean}$. As a direct consequence, the peak linear displacement demands became the same for all time histories.

The scaling described above corresponds to the question brought up in the introduction of the present report: what characteristics of the acceleration time histories influence the SDOF system's displacement or ductility demand, given the same spectral acceleration at the system's natural frequency. Furthermore, the scaling made sure that all ground motions pushed the SDOF system into the non-linear range.

The spectral intensities **SI a** and **SI b** gave the highest correlation coefficients. The discussion that follows focuses therefore on spectral intensities and slope characteristics – as well as on magnitude for comparison. The correlation coefficients obtained for the other characteristics are significantly lower than those found for spectral intensities and slope characteristics. They may be found in (Sharma, 2002).

3.1 Magnitude

Figure 3 shows the correlation between ductility demand and magnitude for R = 3 as a function of the initial natural frequency. The results are poor since the correlation coefficients remain below 0.3. The fact that the coefficients are positive is logical though. Figure 4 highlights the scatter of the ductility demand as a function of magnitude for the 164 time histories.

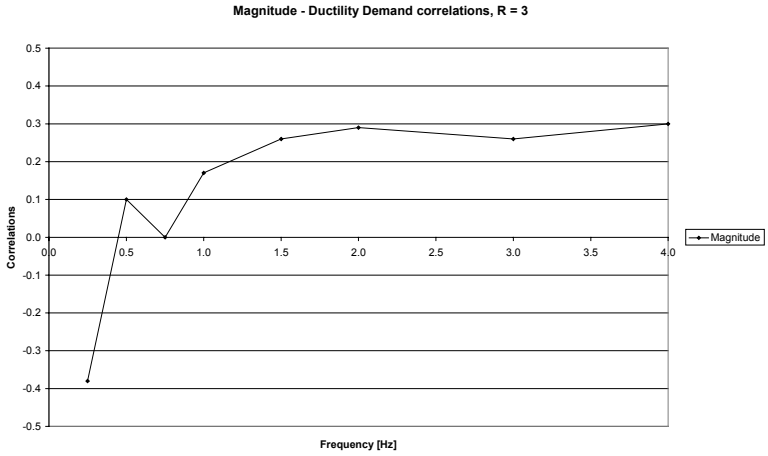

Figure 3: Correlation coefficients between ductility demand and magnitude.

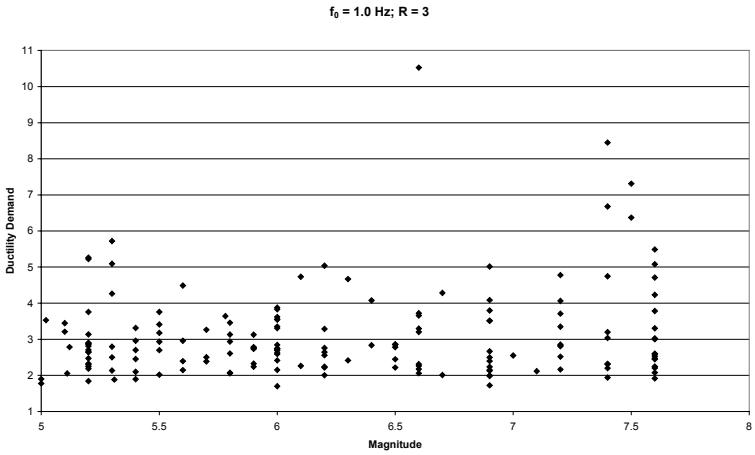

Figure 4: Scatter of the ductility demand as a function of magnitude for f_0 = 1.0 Hz and R = 3. Correlation coefficient r = 0.17.

3.2 Spectral intensities

Figure 5 shows the correlation between ductility demand and spectral intensities for R = 3 as a function of the initial natural frequency. With correlation coefficients constantly between 0.6 and 0.9, the newly defined spectral intensity SI b can be considered as being very satisfactory. Nau & Hall's definition, SI a, yields higher values for frequencies above 1.5 Hz, but shows poor performance below 1.0 Hz. Figure 6 is the counterpart of Figure 4 for a much better characteristic, namely SI b.

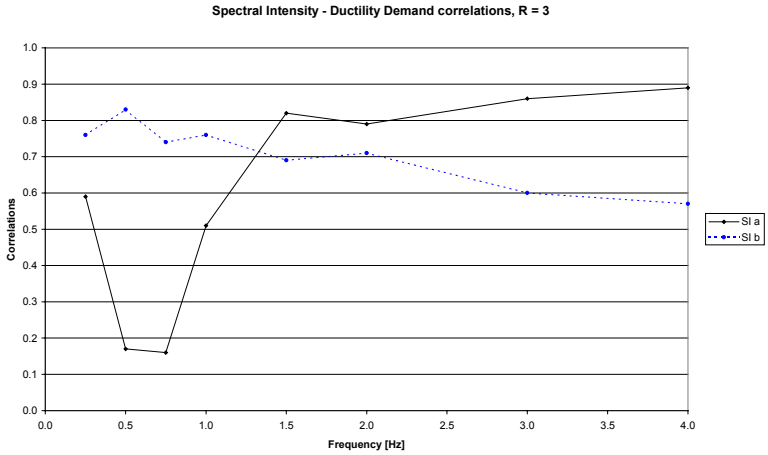

*Figure 5: Correlation coefficients between ductility demand and spectral intensities according to Nau & Hall (**SI a**, straight line) and according to the new definition (**SI b**, dotted line), respectively*

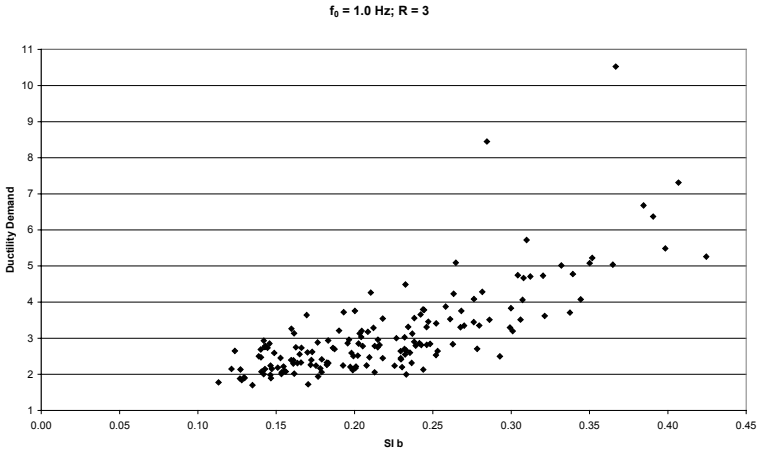

Figure 6: Scatter of the ductility demand as a function of spectral intensity SI b for f_0 = 1.0 Hz and R = 3. Correlation coefficient r = 0.76.

3.3 Slope

Figure 7 shows the correlation between ductility demand and slope for R = 3 as a function of the initial natural frequency. Here, the correlation coefficients are negative, which is plausible. A negative correlation means that the flatter the response spectrum below the initial natural frequency, the higher the expected displacement or ductility demand.

The computations for three different damping ratios show that the best correlation is obtained for a reasonable damping ratio that does neither totally flatten the spectrum nor leaves too many isolated "aleatory" peaks.

The positive correlation that appears for 0.25 Hz is an artefact. The frequency content of most recorded ground motions is unreliable below 0.2 Hz or 0.3 Hz owing to standard high pass filtering that is often applied for base line corrections.

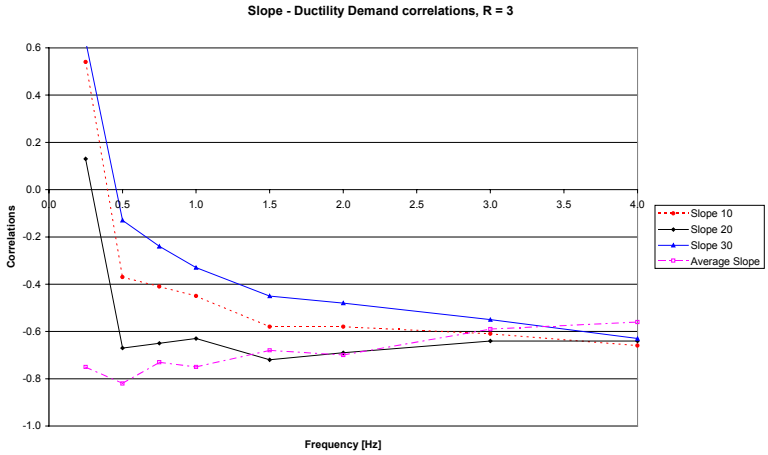

Figure 7: Correlation coefficients between ductility demand and slope for 10 % (dotted line), 20 % (circles) and 30 % (triangles) damping. The results for the average slope (dashed line) are plotted as well.

3.4 Average slope

The correlation between ductility demand and average slope for R = 3 as a function of the initial natural frequency is already shown in Figure 7. It turns out that the average slope gives similar results as the slope for frequencies above 1.0 Hz. However, for lower frequencies, average slope performs much better.

Figure 8 focuses on the differences between the correlation for average slope and the newly defined spectral intensity **SI b**. It was of course necessary to take the absolute values of the average slope correlation coefficients. The results are nearly identical. Nevertheless, it is worth noticing that the spectral intensity seems to give a slightly better correlation.

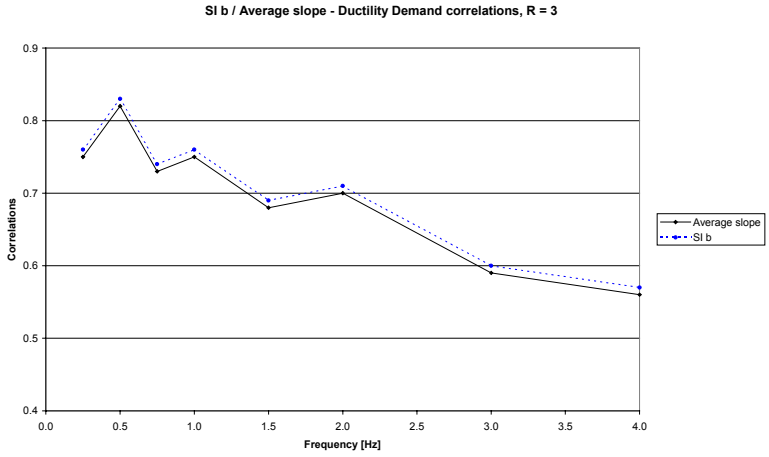

*Figure 8: Correlation coefficients between the average slope (continuous line) and the newly defined spectral intensity **SI b** (dotted line).*

3.5 Conclusions and validation

The main findings obtained so far may be summarised as follows:

- Based on the results presented in section 3 (and appendix A.2), displacement or ductility demand shows the best correlation with the newly defined **spectral intensity SI b**. This result remains also valid if acceleration time histories are used that have different spectral accelerations at the SDOF system's initial natural frequency.
- The correlation with the **average slope $\overline{m}$** characteristic is practically as good as with SI b. However – see section A.7.2 –, average slope is only a valid characteristic if time histories with identical spectral acceleration at the SDOF system's initial natural frequency are compared.
- For unscaled time histories featuring quite different spectral accelerations, the classical **spectral acceleration S_a** still gives a rational indication of the "severeness" of the earthquake ground motion.

Validation tests were carried out in order to confirm the facts highlighted above. A SDOF system, defined by its initial natural frequency f_0 and its expected strength reduction factor R, was submitted to two specific types of ground motions: synthetic and recorded time histories. The entire validation may be found in appendix A.8. The related findings, reported below, clearly confirm the facts found so far.

By confronting the ranking of the time histories, on the one hand based on displacement or ductility demand found by non-linear analysis, and on the other hand based on the different earthquake characteristics, it is possible to make the following statements:

- The newly defined spectral intensity SI b always gives the best results.
- The classical spectral acceleration characteristic S_a is not so bad – it figures out about 2 of the 3 worst cases. This performance is however largely tributary to the fact that large acceleration peaks occur in a set of recorded earthquakes.
- The average slope $\overline{m}$ characteristic is mostly efficient for small strength reduction factors and at low frequencies since the integration interval remains small and the influence of local peaks in the spectrum is fully taken into consideration.

4. Fling

The final part of this research project was devoted to a recent open question in engineering seismology and earthquake engineering: the impact of "fling" on structural behaviour. Fling is a strong velocity pulse that results from the permanent tectonic ground displacement that corresponds to the slip on the causative fault. Fling was recently observed in the near fault ground motions of the 1999 Kocaeli (Turkey) and Chi-Chi (Taiwan) earthquakes.

Figure 9 shows the TCO 052 E recording of the Chi-Chi earthquake in its original version, i.e. with fling, and after extraction of the fling, i.e. without fling. A strong velocity pulse corresponding to a step in displacement can clearly be observed in the original recording. In acceleration, the fling corresponds to one period of more or less a sinus function, but little can be seen of this in the acceleration time history. Note that the algorithm used for the computation of the SDOF system's ductility

demand did not converge for this time history; this was probably due to the strong fling present in the TCO 052 E recording.

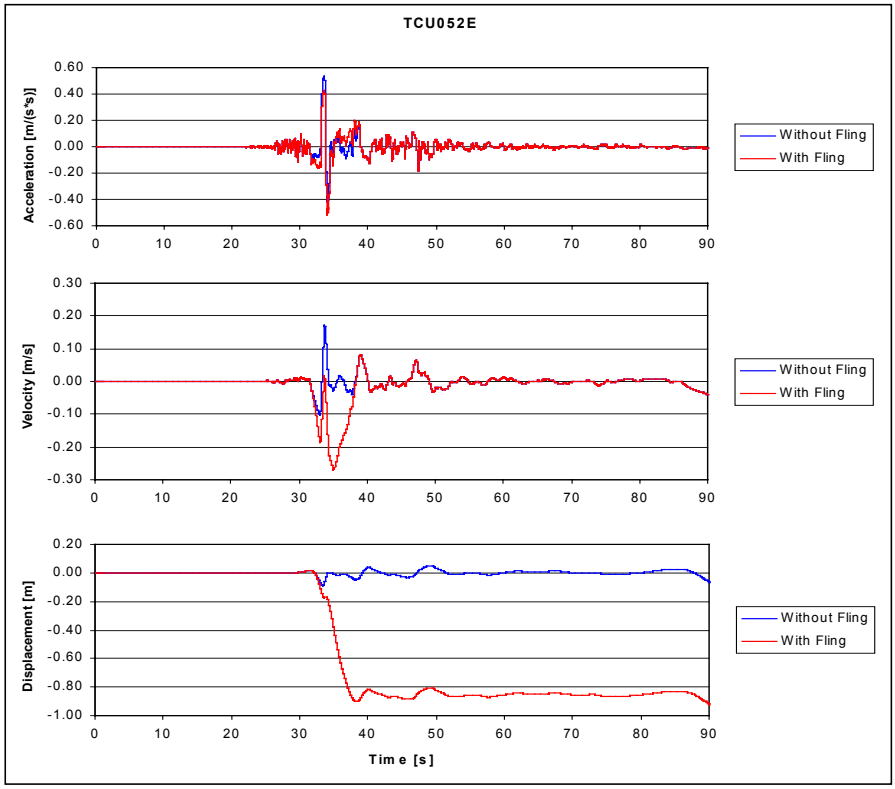

Figure 9: TCO 052 E recording of the Chi-Chi (1999) earthquake with fling and after extraction of the fling: a strong velocity pulse as well as a kind of step function for the displacement can be seen.

Up to now, research on fling seems to be limited to the seismological community; the impact of fling on structural behaviour has not yet been studied. In order to guide their future research, the seismologists would like to know from the engineers whether fling significantly influences structural behaviour or not.

4.1 Methodology

As a very preliminary study, 18 recordings (acceleration time histories) of the Chi-Chi earthquake containing fling were applied to the SDOF systems. Then, the same recordings, after "manual" extraction of the fling, were applied again to the same SDOF systems. The displacement or ductility demands were calculated for the time histories with and without fling, and the results were compared with each other.

The set of 18 recordings was not homogenous in the sense that the amplitude of the fling strongly varied from one case to the other.

The seismic structural responses were computed with the Takeda model and for four strength reduction factors: R = 2, 3, 4 and 5. Since fling has a relatively low frequency content, only initial natural frequencies ranging from f_0 = 0.25 Hz to f_0 =

2 Hz were considered. In order to focus on fling only, the yield displacement of the SDOF systems was kept constant for each recording with and without fling and was equal to the mean value of the related spectral displacements, divided by the strength reduction factor R.

4.2 Results and conclusions

In many cases, rather small differences in the displacement or ductility demand resulted from the time histories with and without fling. In fact, many of the earthquake recordings that were used only contained a relatively weak fling. The detailed results are shown graphically in Appendix A.9.

Where significant differences occurred, they were limited to the lowest frequency domain (< 1 Hz), as can be expected from the low frequency character of flings. The differences tended to increase with the level of the strength reduction factor R. Surprisingly, where differences occurred, larger displacement or ductility demands resulted for the recordings *without* fling, except for one single case. The reasons for this peculiar result are not understood. The calculations were carefully checked in order to make sure that there was no confusion between the cases with and without fling.

Figure 10 presents the differences in ductility demand, $\Delta(\mu_\Delta)$ (ductility demand without fling minus ductility demand with fling), as a function of the fling amplitude in acceleration for the case of R = 3. The $\Delta(\mu_\Delta)$ given in Figure 10 corresponds to the maximum difference, irrespective of frequency, that could be found. A relatively poor correlation can be observed, with nevertheless a rough tendency of larger $\Delta(\mu_\Delta)$ for stronger flings.

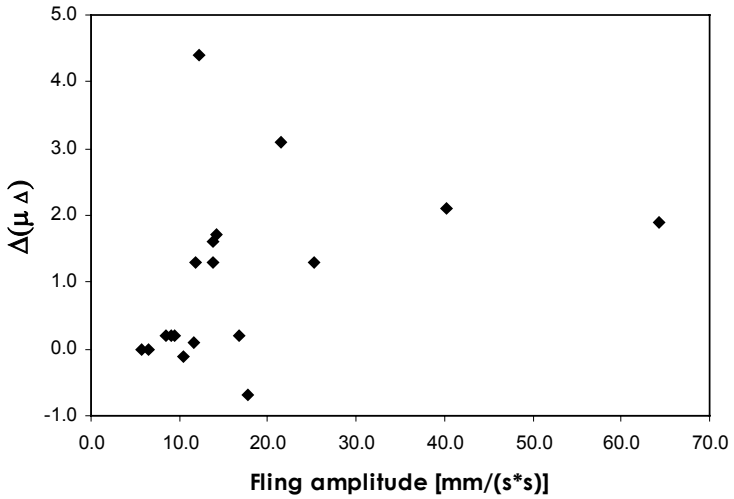

Figure 10: Ductility demand without fling minus ductility demand with fling, $\Delta(\mu_\Delta)$, as a function of the fling amplitude in acceleration for R = 3

The limited number of recordings used in this investigation does not yet allow to draw general conclusions, particularly in view of the counterintuitive results. Much more research work is necessary to understand the impact of fling on RC structures.

5. Recommendations

The following recommendations are based on the present study of ductile RC SDOF systems. Therefore, they can be expected to be valid for structures that can reasonably be modelled as SDOF systems. The behaviour of more or less regular ductile RC structures is usually well approximated by SDOF models. More research work, however, would be necessary in order to further develop and test these recommendations for strongly irregular RC structures that behave more like multi-degree of freedom systems.

The following recommendations can be given for the choice of acceleration time histories to be used for non-linear seismic analyses:

- The spectral acceleration S_a of the acceleration time history should be equal or close to the spectral acceleration of the given design spectrum at the initial fundamental period T_0 of the structure under study and, as far as possible, within the range between T_0 and the period Ts, Ts being the fundamental period that corresponds to the secant stiffness for either the expected ductility demand or the design ductility.
- The "severeness" of several time history candidates that fulfil the above conditions can be ranked with the aid of the newly defined spectral intensity SI b: the larger SI b, the higher the displacement and ductility demand. It is up to the structural engineer to decide whether to use the most "severe" time histories for worst case studies or to use time histories that have neither particularly high nor particularly low values of SI b.

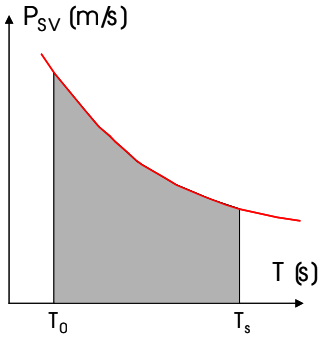

$$SI\ b\left(\zeta, T_0, R\right) = \frac{1}{T_s - T_0}\int_{T_0}^{T_s} P_{SV}\left(\zeta\right)\cdot dT\,, \qquad \zeta = 5\%\,,$$

where $T_s = T_0 \cdot \sqrt{R} = \frac{\sqrt{R}}{f_0}$

P_{SV} is the pseudo-velocity spectrum and ζ the damping ratio. T_0 is the initial natural period and T_S corresponds to the secant stiffness. R is the strength reduction factor.

6. Project significance

Seismic design, control and upgrade is of growing economic importance in Switzerland:

- several cantons (Valais, Basel, Aargau, Berne, etc.) have launched a seismic control and upgrading program for their important structures
- the Swiss Confederation has started its own seismic control and upgrading program
- about three years ago, an agreement was signed between the public authorities and the chemical industry in Basel for a systematic check and upgrade of safety relevant buildings and installations

– some important national and international companies have started their own seismic program in order to limit production loss in case of an earthquake (example: Lonza Ltd, Basel/Valais)

As is generally recognised, the seismic risk is particularly important for existing structures. Around 90 % of the structures that exist today were built according to ancient codes that did not yet take into account seismic safety in an adequate manner. Therefore, an important, but unknown number of structures do not correspond to current seismic safety standards.

For particularly important RC structures, as well as for checking simplified methods of seismic evaluation, it is expected that more and more non-linear seismic analyses will be performed in the future. The results of the present research project allow to choose the acceleration time histories needed for such calculations in a more rational manner than before. As a by-product, the "severeness" of earthquake recordings with respect to a given RC structure can be evaluated with the aid of the newly defined spectral intensity SI b.

7. Acknowledgements

This research project lasted 9 months starting from December 2002. It was supported by the Foundation for Applied Research in Concrete of Cemsuisse. This financial support is gratefully acknowledged.

The project partners are grateful to Dr Norman Abrahamson. He made available to the project the Chi-Chi Taiwan earthquake recordings with fling as well as the versions with extracted fling.

8. References

Allahabadi R., Powell G.H. (1988). *Drain-2DX User Guide*. Report No, UCB/EERC-88/06. College of Engineering, University of California, Berkeley 1988.

Bommer J. J., Martinez-Pereire A. (1999). *The Effective Duration of Earthquake Strong Motion*. The Journal of Earthquake Engineering 1999; Vol. 3 No. 2

Elenas A. (2002). *Seismic Damage Potential Described by Spectral Intensity Parameters*. 12th European Conference on Earthquake Engineering. Paper 267. London 2002.

EC8 – Eurocode 8 (2002). *Design of Structures for Earthquake Resistance, Part 1: General Rules, Seimic Actions and Rules for Buildings, prEN 1998-1*; Draft 5, May 2002; Europäisches Komitee für Normung (CEN), Brüssel; 197 pp.

Lestuzzi P. (2000). *Dynamisches plastisches Verhalten von Stahlbetontragwänden unter Erdbebeneinwirkung.* Dissertation ETH Nr. 13726, Zürich, 2000.

Lestuzzi P., Badoux M. (2003). *The γ-Model : a simple hysteretic model for reinforced concrete walls.* Proceedings of the fib-Symposium; Concrete Structures in Seismic Regions, Athens 2003.

Musson R.M.W. (2002): *Effective Peak Acceleration as a Parameter for Seismic Hazard Studies.* 12th European Conference on Earthquake Engineering. Paper 32. London 2002.

Nau M., Hall W.J. (1984). *Scaling Methods for Earthquake Response Spectra.* Journal of Structural Engineering 110 (7) pp 1533-1548, 1984.

Saactioglu M. (1991). *Modeling hysteretic force deformation relationships for R/C elements.* Earthquake-Resistant Concrete Structures.: Inelastic Response and Design. Special publication SP-127 of the American Concrete Institute (ACI). Detroit, Michigan. April 1991.

Sabetta F., Pugliese A. (1996). *Estimation of Response Spectra and Simulation of Nonstationary Earthquake Ground Motions.* Bulletin of the Seismological Society of America, Vol 86, No.2, pp. 337-352, April 1996.

Saiidi M., Sozen M.A. (19981). *Simple nonlinear seismic analysis of R/C structures*. Journal of the Structural Division. Proceedings of the American Society of Civil Engineers (ASCE). Vol. 107, No. ST5. May 1981.

Sharma S. (2002) *Non-linear Dynamic Response of Structures Subjected to Recorded Earthquakes.* Internship project IIT-EPFL, December 2002.

Smit P. et al. (2002). *European Strong Motion Database*. European Council, Environment and Climate Research Program, 2000.

Takeda T., Sozen M.A., Nielsen N.N. (1970). Reinforced concrete response to simulated earthquakes. Journal of the Structural Division. Proceedings of the American Society of Civil Engineers (ASCE). Vol. 96, No. ST12. December 1970.

Appendices A.1 to A.9

A.1 Hysteretic models

The force-displacement relationships defining the six hysteretic models that were considered in the project are plotted in the figure below.

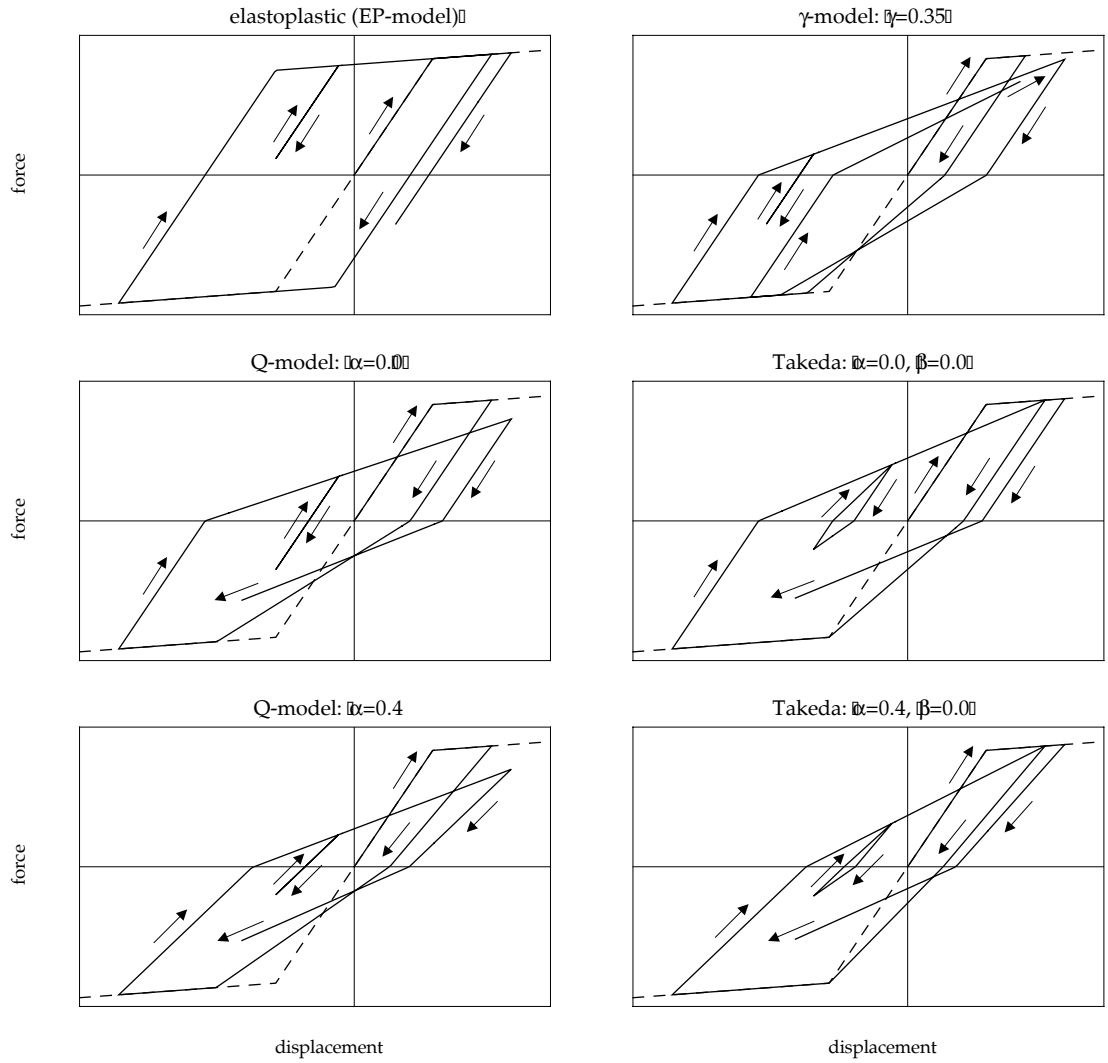

Figure A.1.1: The six hysteretic models that were used in the present research project

Elastoplastic model: The elastoplastic model (EP-model) is sometimes also called bi-linear model. Even if it is mainly intended for elastoplastic material, such as steel, this model is intensively used for all types of materials because of its simplicity. The force-displacement relationships of the EP-model are totally specified through three parameters: the stiffness, the yield displacement and the post yield stiffness expressed as a portion of the stiffness. For the simulation of reinforced concrete, the main default of the EP-model is the too stiff reloading curve after yielding and unloading. This characteristic does not take into account the closure of the cracks. It leads to excessive energy dissipation by the inelastic cycles and to unrealistic permanent deformations.

Gamma model: According to Lestuzzi et al. (2003), the EP-model is modified with a condition for the reloading curves specified by a supplementary parameter γ. For large yield excursions (displacements greater than current peak displacement), the reloading curves cross the elastic portion of the envelope at a height of 1-γ of the yield force. Otherwise (displacements smaller than current peak displacement), the reloading curves aim for the current peak displacement. The force-displacement relationships of the γ-model are specified through four parameters: the stiffness, the yield displacement, the post yield stiffness and γ. The value of γ has to be determined empirically. Similar to the EP-model, the γ-model does not consider stiffness degradation due to increasing damage. The name of the model reflects the shape of the produced hysteretic loops, which looks like the symbol γ.

Takeda model: Since the Takeda-model includes realistic conditions for the reloading curves, it provides a much better simulation of the features of reinforced concrete in comparison with the EP-model. Moreover, the Takeda-model takes into account the degradation of the stiffness due to increasing damage, which is an important feature of reinforced concrete subjected to seismic action (Saatcioglu, 1991). However, the Takeda-model does not include strength degradation.

The Takeda-model was initially proposed in a basic version by Takeda et al. (1970) and was adapted afterwards through many authors. The version used here is the one of Allahabadi et al. (1988). The force-displacement relationships of the Takeda-model are specified through five parameters: the initial stiffness, the yield displacement, the post yield stiffness, a parameter relating the stiffness degradation and another specifying the target for the reloading curve. Different rules are used for large and for small hysteretic cycles. The small cycles are, one more time, divided into small cycles with yielding and small cycles with small amplitudes.

Takeda model (zero): This model considers a specific and simple case of Takeda model where $\alpha = 0$ i.e. no degradation of the unloading stiffness is taken into account.

Q model: A simplified version of the Takeda-model was proposed by Saiidi et al. (1981), the Q-model. In comparison with the Takeda-model, the consideration of the absolute value of peak displacement for both directions constitutes the main simplification. Moreover, there are no distinctions between large and small hysteretic cycles. The reloading curves systematically target the point corresponding to the absolute value of actual peak displacement.

Similar to the Takeda-model, the Q-model takes into account the stiffness degradation, but does not take into account the strength degradation. The force-displacement relationships of the Q-model are totally specified through four parameters: the initial stiffness, the yield displacement, the post yield stiffness and a parameter relating the stiffness degradation.

Q model (zero): this model proceeds assuming the factor $\alpha = 0$ and hence does not consider the degradation of the unloading stiffness.

The displacement and the ductility demands were computed for each of the six hysteretic models. Apart from the elastoplastic model, whose simplistic modeling of RC elements leads to a general underestimation of the ductility demand, they all yielded very similar ductility demands. It was therefore decided to focus on the Takeda model for the interpretation of the results.

A.2 Correlation coefficients for original earthquake recordings

This chapter discusses the situation when the original acceleration time histories with very different levels of spectral acceleration are applied to the SDOF systems.

A.2.1 Scatter of the recorded earthquakes' spectral values

Since the 164 spectral displacement values S_d are very scattered as shown in figure A.2.1, plus having in mind how the structures are defined (see below), it should not be surprising that there are earthquakes that do not drive the structure into the non-linear range.

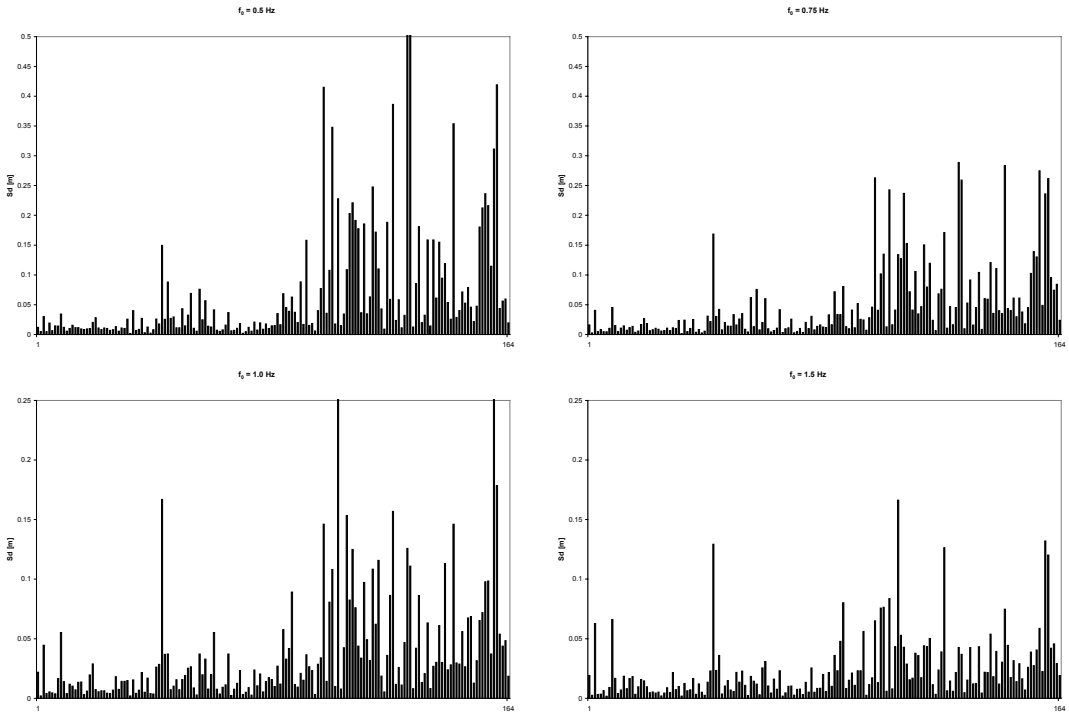

Figure A.2.1: Scatter of the spectral displacements of the 164 time histories at four frequencies: 0.5 Hz, 0.75 Hz, 1.0 Hz and 1.5 Hz.

Indeed, if $S_{d,i} \leq \frac{S_{d,mean}}{R}$, the structure will remain elastic under the action of that particular earthquake. Table A.2.1 shows how many earthquakes actually trigger a plastic behavior of the structure.

Table A.2.1: Number of earthquakes – out of 164 – that lead to a plastic behavior of the structure

	0.25 Hz	0.5 Hz	0.75 Hz	1.0 Hz	1.5 Hz	2.0 Hz	3.0 Hz	4.0 Hz
R = 2	66	71	82	89	98	102	119	132
R = 3	88	86	96	109	117	126	141	151
R = 4	94	100	110	122	130	141	157	162
R = 5	102	112	125	132	139	151	161	164

The results for the characteristics examined with the original earthquakes are presented and illustrated by a single graph as far as the differences with respect to

the various strength reduction factors remain small. The complete results are given in the appendix A.3 to A.7.

A.2.2 Spectral acceleration

Figure A.2.2 shows the correlation coefficients for R = 3 for both the set of 164 earthquake recordingss and a restricted set – between 86 and 151 time histories according to table A.2.1 – containing only those that set off a non-linear behavior. The correlation coefficients are very high for very low frequencies, but become quickly somewhat lower for stiffer structures. Contrary to one's intuition, the correlation coefficients are lower for the restricted set of earthquake recordings.

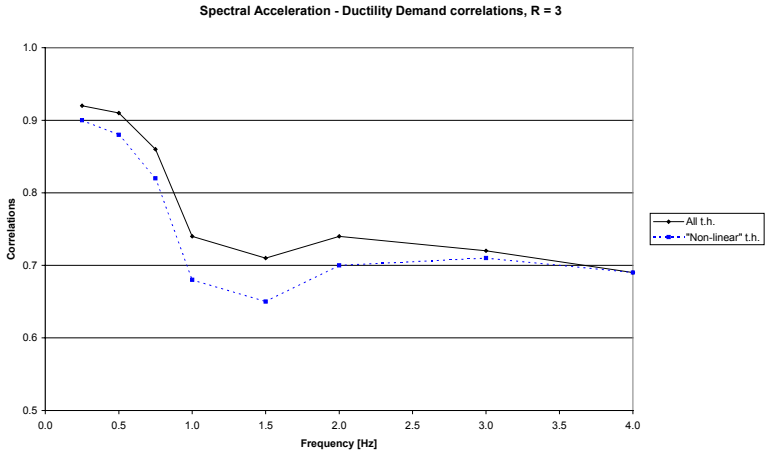

Figure A.2.2: Correlation coefficients between the ductility demand and the spectral acceleration for the 164 time histories (straight line) as well as for a set restricted to the earthquakes that actually trigger a structural non-linear behavior (dotted line).

The earthquake recordings that let the structure elastic are obviously perfectly correlated (r = 1.0) to the ductility demand. For recordings featuring different spectral accelerations at the SDOF system's natural frequency, it is not surprising that the ductility demand is closely related to S_a. Hence the idea to check which characteristic of a time history influences the ductility demand when S_a is set constant. This concept is tackled in section 3.

A.2.3 Spectral intensities

Figure A.2.3 shows the correlation coefficients for R = 3 for the two types of spectral intensities examined here. The data are related to the entire set of 164 earthquake recordings.

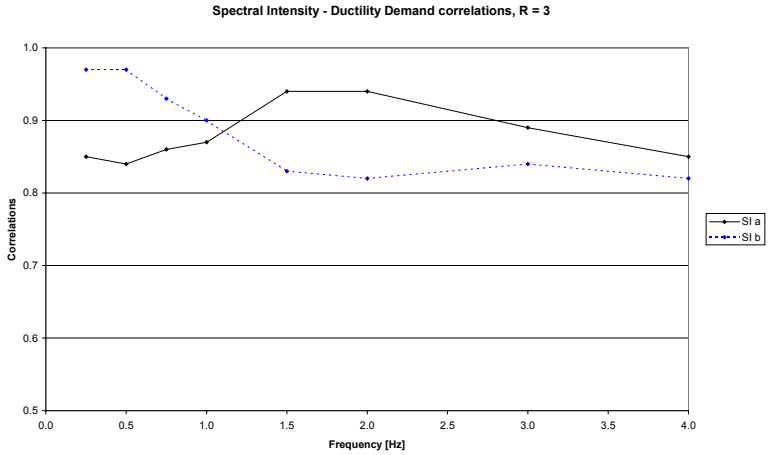

Figure A.2.3: Correlation coefficients between the ductility demand and the spectral intensity according to ***SI a*** *(continuous line) respectively the new definition* ***SI b*** *(dotted line).*

The new definition suggested in the present study improves the correlation coefficients in the low frequency domain. Elsewhere, it becomes less interesting but still shows correlation coefficients superior to 0.8. SIa and SI b can thus both be qualified as reliable characteristics.

A.3 Correlation coefficients for spectral acceleration

The correlation coefficients are plotted in function of the frequencies, for the four strength reduction factors.

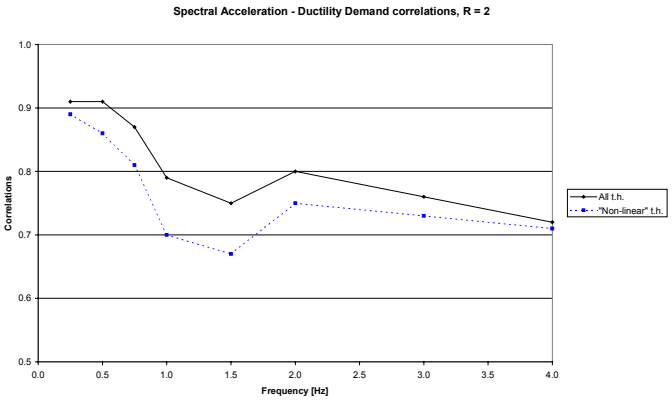

The contiuous lines represent the values for the 164 **original earthquakes**, while the dotted ones illustrate the cases when only those earthquakes that lead the structure into the non-linear range are considered.

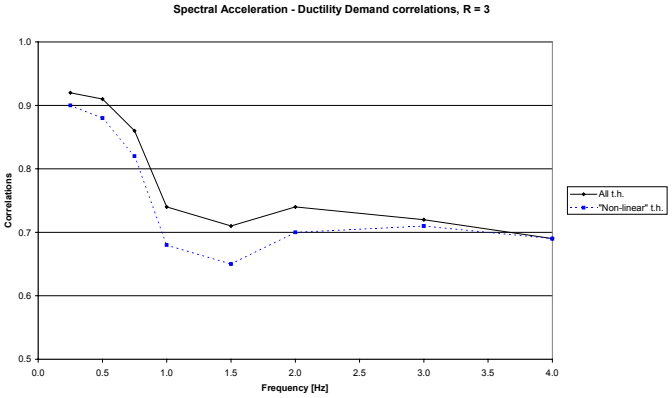

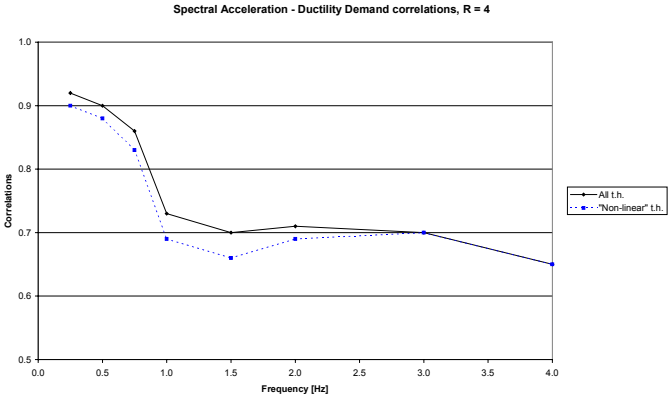

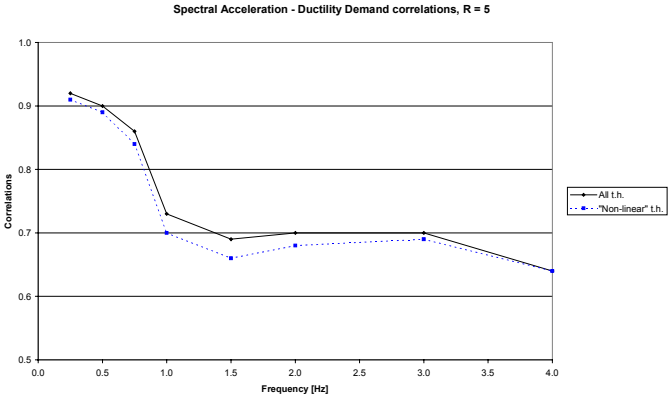

A.4 Correlation coefficients for magnitude

The correlation coefficients are plotted in function of the frequencies, for the four strength reduction factors.

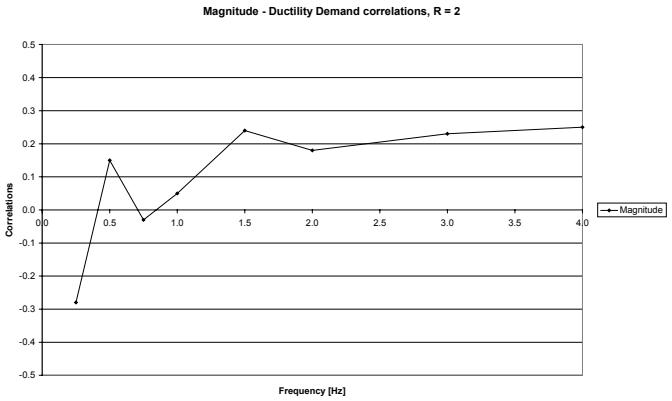

The results are given for the **164 scaled earthquake recordings** (i.e. all recordings are scaled in such a manner that the value of S_a at the SDOF system's natural frequency is identical).

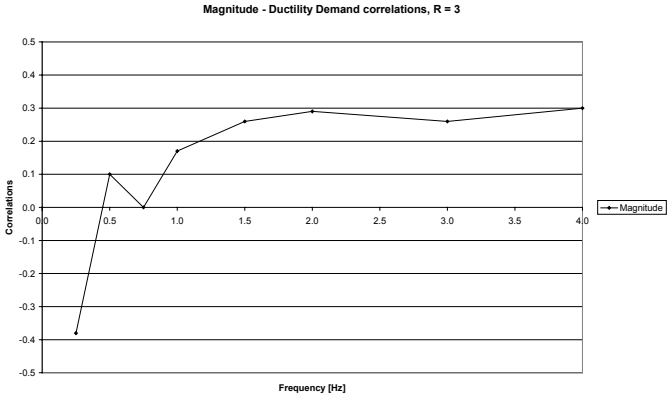

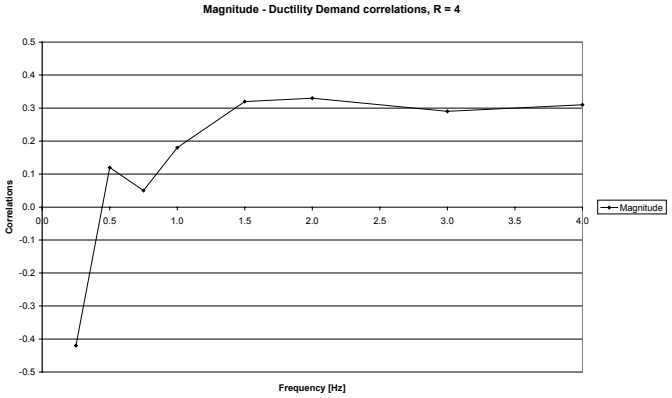

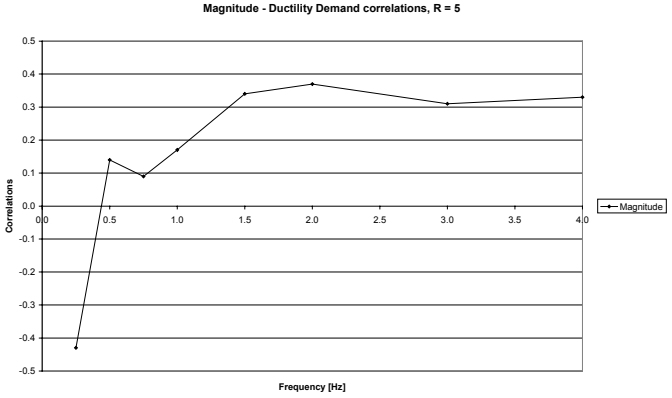

A.5 Correlation coefficients for spectral intensities

A.5.1 Original earthquake recordings: bias

The correlation coefficients are plotted in function of the frequencies, for the four strength reduction factors.

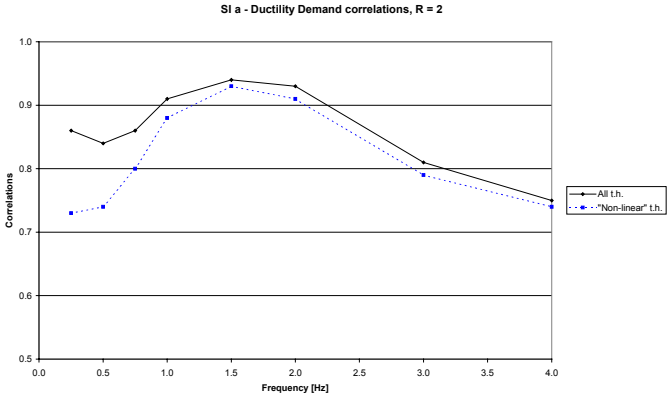

The data are those for the spectral intensity according to Nau & Hall.

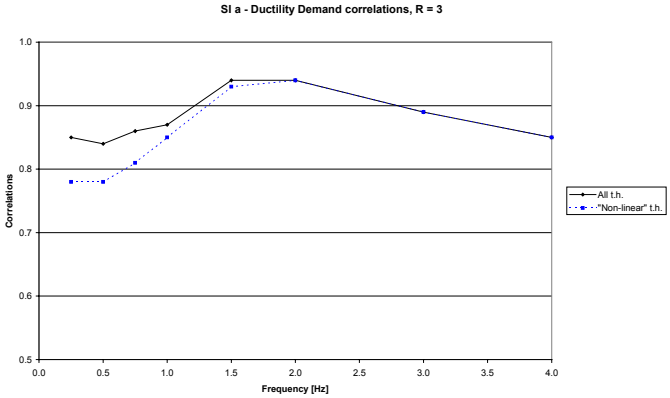

The continuous lines represent the values for the whole set of 164 time histories.

The dotted lines illustrate what happens when only the earthquakes that trigger a plastic behavior of the structure are considered.

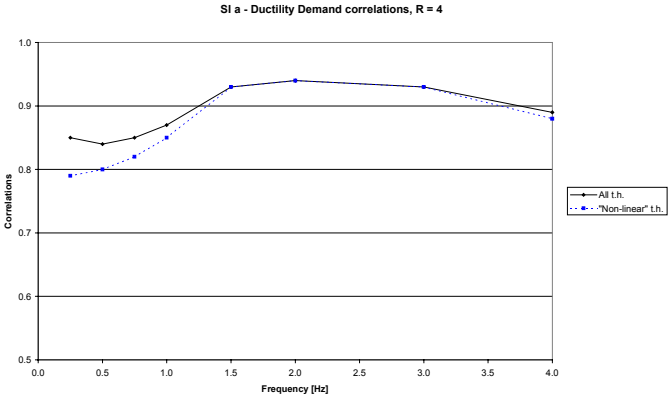

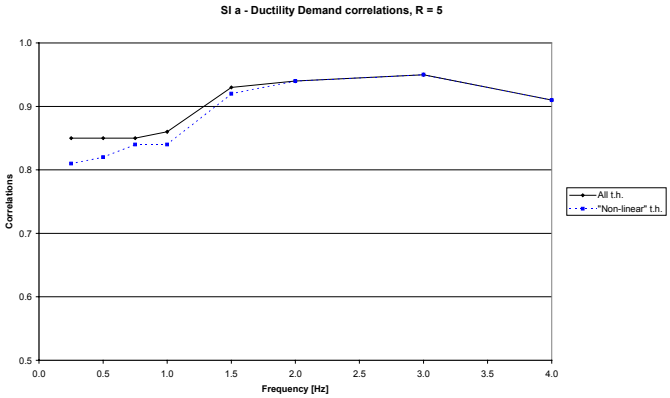

A.5.2 Original earthquake recordings

The correlation coefficients are plotted in function of the frequencies, for the four strength reduction factors.

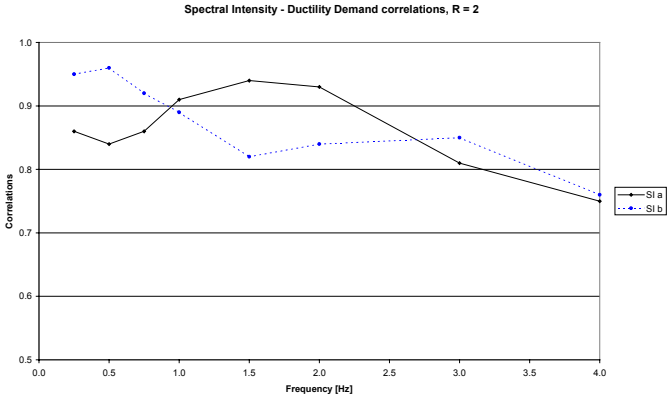

The results are given for the 164 **original earthquake recordings**.

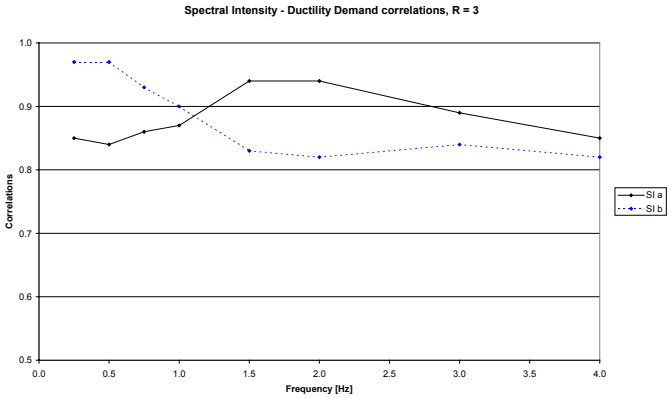

The continuous lines represent the values of SI a according to Nau & Hall.

The dotted lines illustrate what happens when the newly suggested definition, SI b, is used.

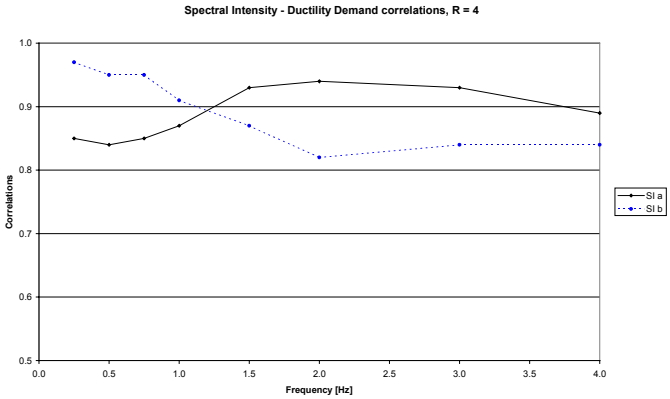

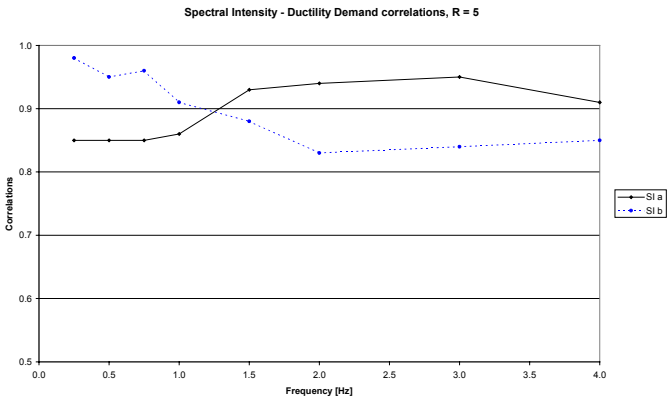

A.5.3 Scaled earthquake recordings

The correlation coefficients are plotted in function of the frequencies, for the four strength reduction factors.

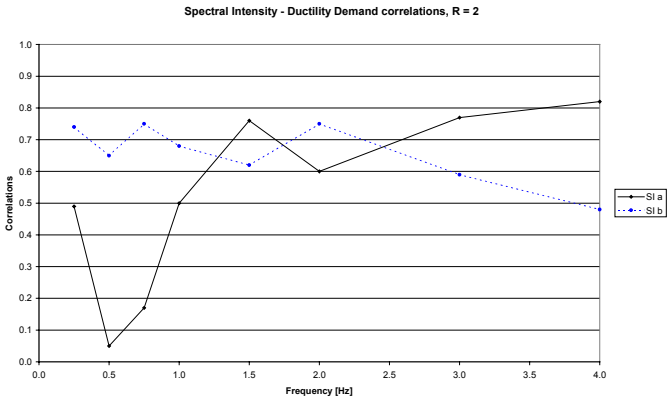

The results are given for the **164 scaled earthquake recordings** (i.e. all recordings are scaled in such a manner that the value of S_a at the SDOF system's natural frequency is identical).

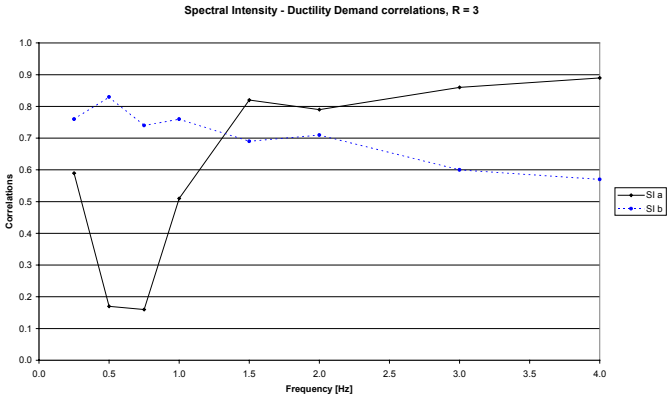

The contiuous lines represent the values of SI a according to Nau & Hall.

The dotted lines illustrate what happens when the newly suggested definition, SI b, is used.

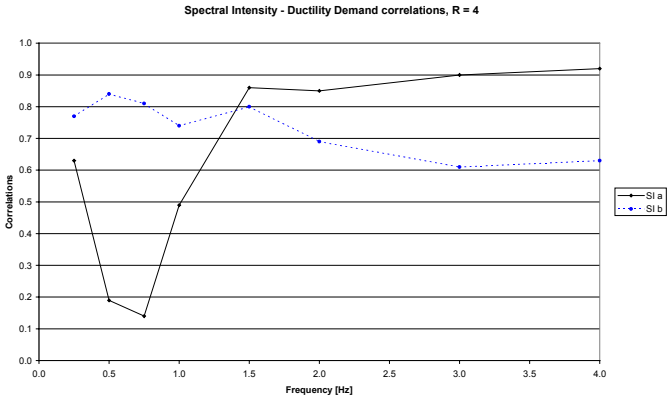

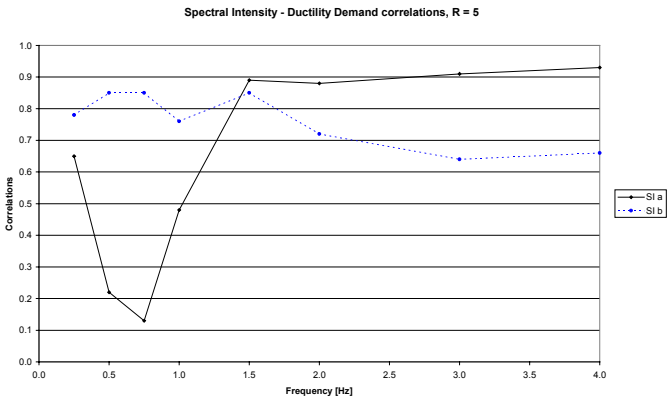

A.6 Correlation coefficients for slope

The correlation coefficients are plotted in function of the frequencies, for the four strength reduction factors.

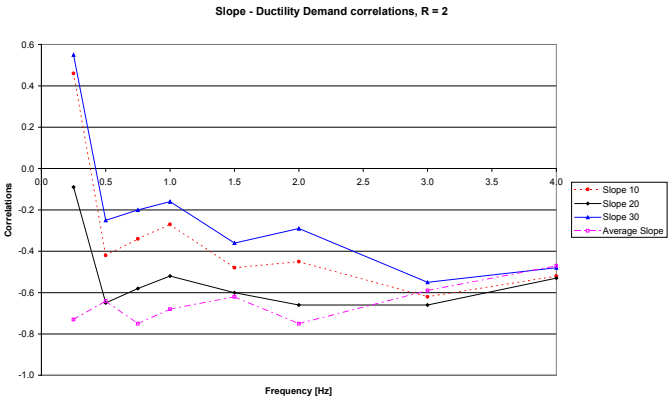

The results are given for the **164 scaled earthquake recordings** (i.e. all recordings are scaled in such a manner that the value of S_a at the SDOF system's natural frequency is identical).

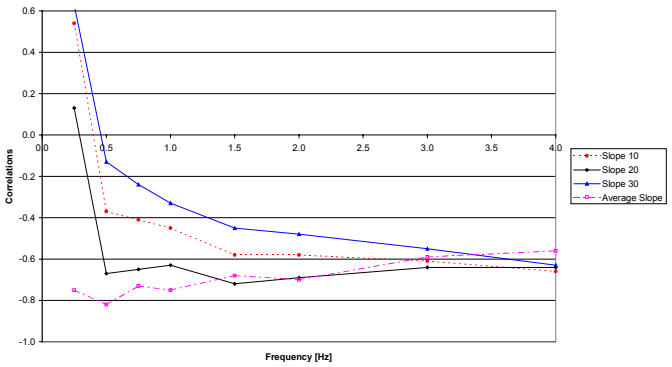

The first three types of curves differ by the percentage of critical damping, set as ζ = 10, 20 and 30 %.

The dashed curves illustrate the results when the average slope is considered.

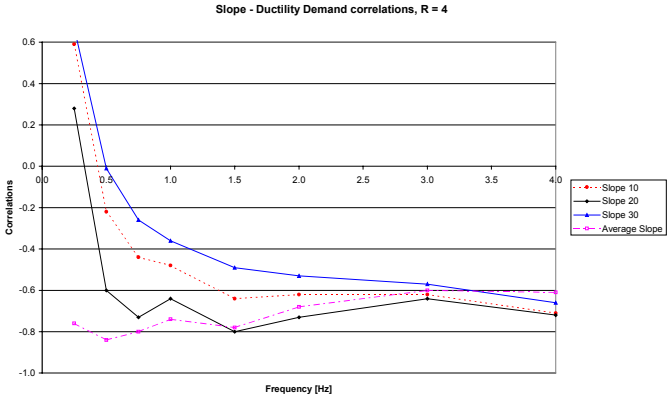

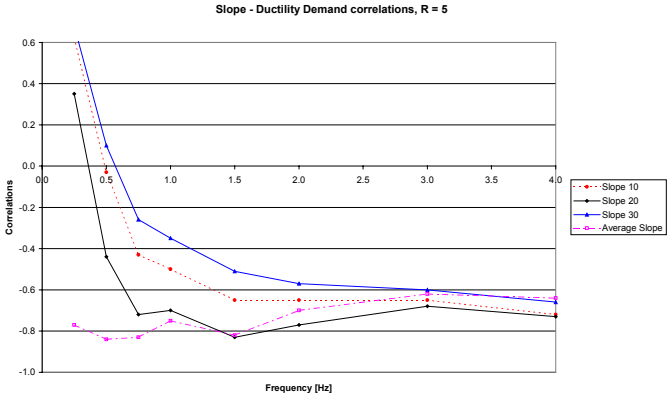

A.7 Correlation coefficients for average slope

A.7.1 Scaled earthquake recordings

The correlation coefficients are plotted in function of the frequencies, for the four strength reduction factors.

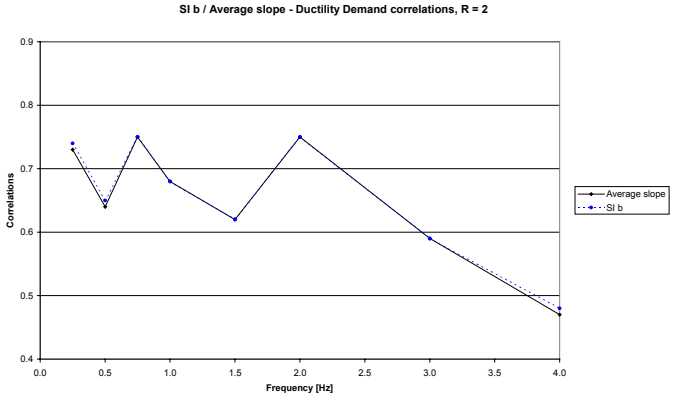

The results are given for the **164 scaled earthquake recordings** (i.e. all recordings are scaled in such a manner that the value of S_a at the SDOF system's natural frequency is identical).

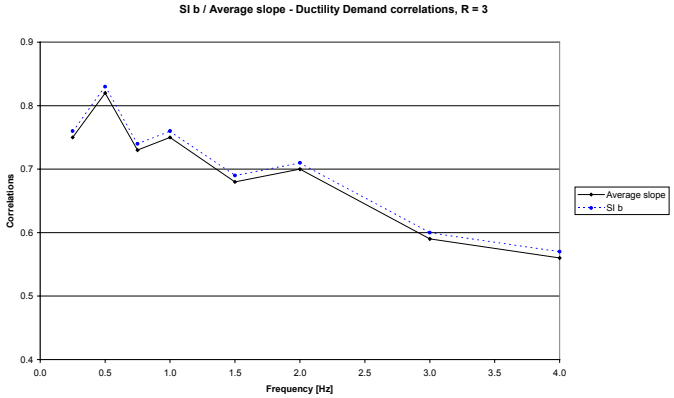

The straight lines represent the absolute values for the average slope.

It makes thus sense to present them in a unique graph along with the results for SI b.

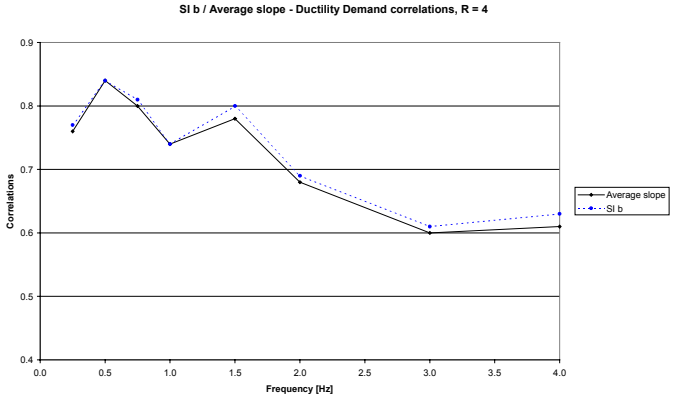

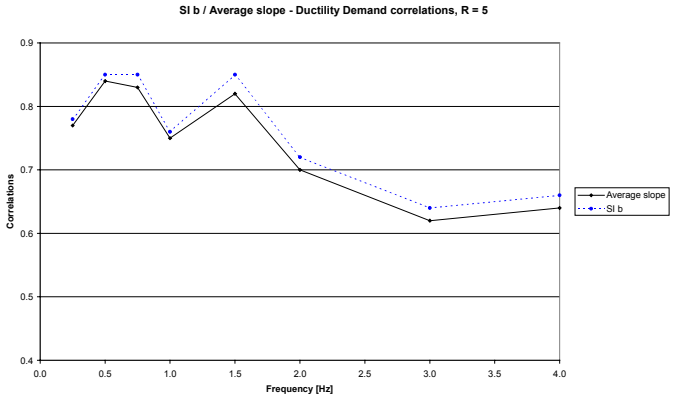

A.7.2 Original earthquake recordings

The correlation coefficients are plotted in function of the frequencies, for the four strength reduction factors.

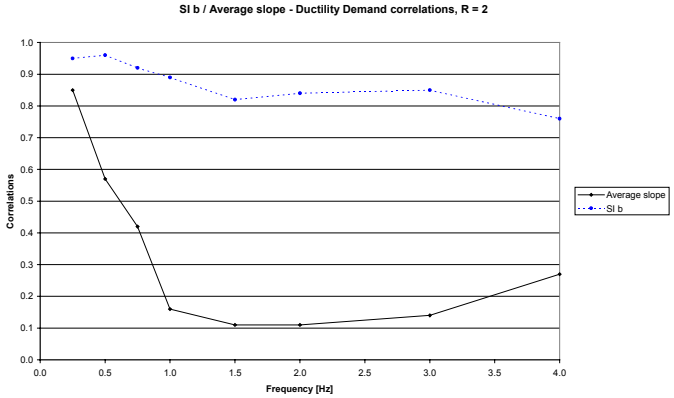

The results are given for the 164 **original earthquakes**.

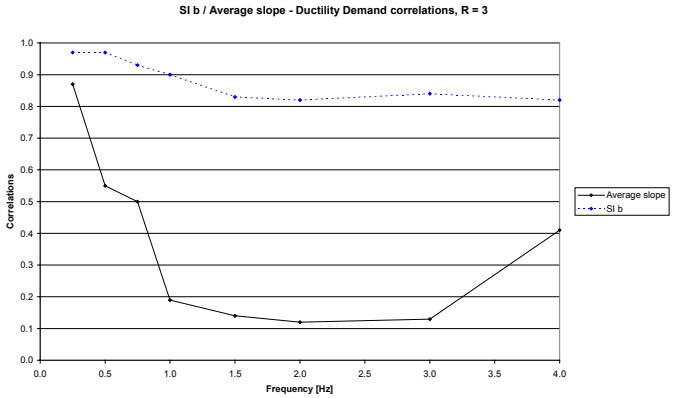

The continuous lines represent the absolute values for the average slope.

It makes thus sense to present them in a unique graph along with the results for SI b.

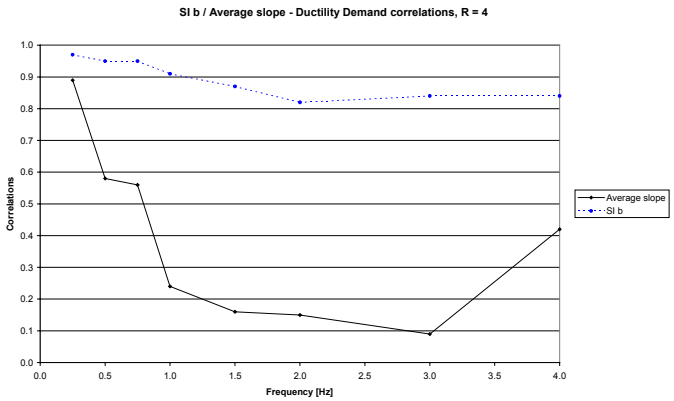

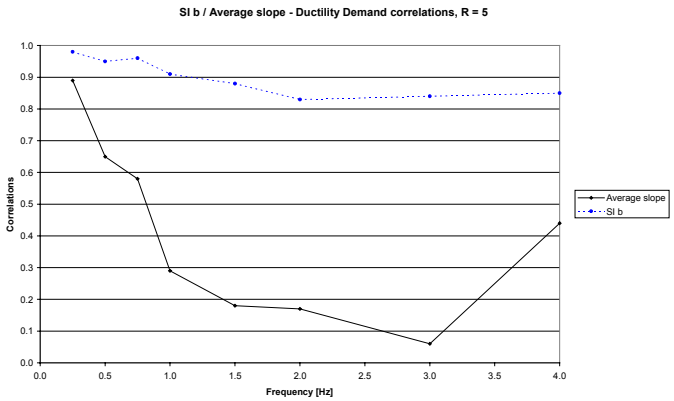

A.8 Validation

Before validation tests are presented, the main findings obtained so far are recalled:

- In order to estimate the displacement or ductility demand of acceleration time histories with very different response spectra, the classical **spectral acceleration S_a** at the SDOF system's natural frequency is a good characteristic, especially in the low frequency domain.
- Based on the results presented in appendix A.2 and in chapter 3, it seems that predicting the ductility demand of a couple of acceleration time histories is best performed by the newly defined **spectral intensity SI b**. This is true for time histories with different as well as with equal spectral accelerations at the SDOF system's natural frequency
- The **average slope $\overline{m}$** characteristic is only efficient for scaled time histories – see section A.7.2 – and should therefore be considered as a confirmation characteristic at disposal for groups of time histories with identical spectral acceleration at the SDOF system's natural frequency.

A.8.1 Goal

The objective is to check whether the facts highlighted above remain true when submitting a SDOF system, defined by its initial fundamental frequency f_0 and its expected strength reduction factor R, to two specific types of ground motion.

A.8.2 Synthetic time histories

Structural engineers without specific seismological knowledge may feel more confident with the use of synthetic earthquakes, which can be processed so as to match design demands. The best – producing non-stationary time histories – simulation method available today is the one developed by Sabetta et al. (1996). Besides, the use of synthetic earthquakes that differ only by their phases enables the generation of different sets of time histories displaying the same spectral mean value at a given frequency. The question raised in appendix A.2 can thus be tackled.

Two sets of ten time histories, featuring an average spectral value contained in a 10% interval around a given spectral value – $S_{a,mean}$ of the database at 1.0 Hz – are processed. The slope at 1.0 Hz for the set A – magnitude 7.0, epicentral distance 50 km – is flatter than for the set B – magnitude 5.9, epicentral distance10 km – as shown in figure A.8.1.

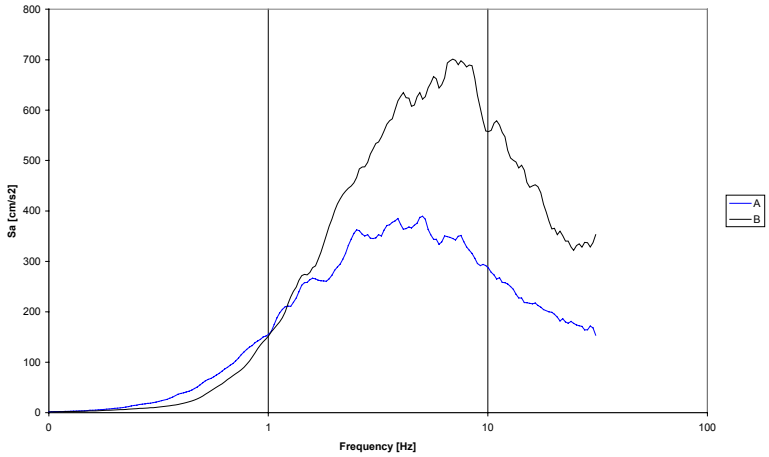

Figure A.8.1: Average acceleration spectra for set A and B

The non-linear response and the values of the earthquake characteristics are computed. Their averages are given below.

For f_0 = 1.0 Hz and R =5.0

Set	μ_Δ	*SI a*	*SI b*	$\overline{m}$
A	*4.60*	*23.4*	*21.2*	*241.2*
B	*3.90*	*21.2*	*14.9*	*316.7*

It appears that all three examined characteristics catch the difference between the two sets of earthquakes. This little example shall just be viewed as a basic confirmation since the analysis is based on averages.

A.8.3 Recorded time histories

The spectrum valid for zone 3a – PGA = 1.3 m/s^2 – for a soil of type B according to SIA 261 is chosen. Such conditions are for example encountered in Basel. Ten time histories are extracted from the database. The selection was performed in a way that a validation of the suggested characteristics could be carried out. This means in particular that the boundaries used to select the time histories were rather loose. Figure A.8.2 shows the corresponding response spectra along with their mean value.

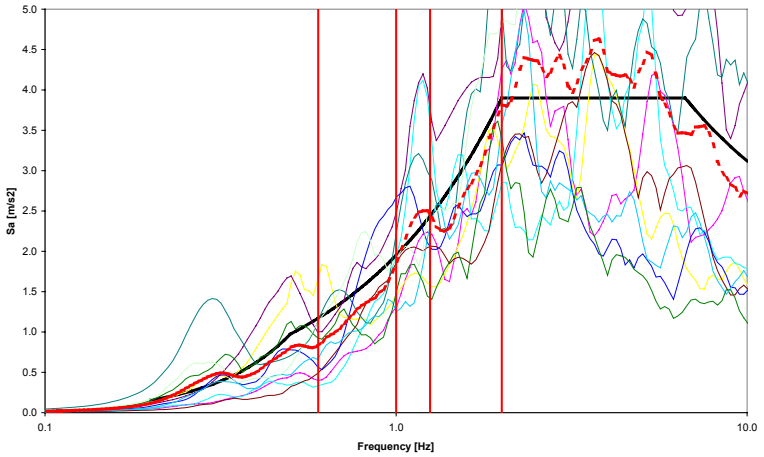

Figure A.8.2: Response spectra of the ten selected recorded time histories used for the validation of the suggested characteristics. The average spectrum as well as the design spectrum are plotted too. The vertical lines represent the frequencies for which validation computations were performed.

The time histories are ranked by decreasing ductility demand. The three worst values – i.e. those that are expected to identify the most demanding time histories – are printed in bold. The darker the shading, the more demanding is the time history.

For f_0 = 0.6 Hz and R =4.0

Quake	*177*	*147*	*123*	*187*	*192*	*179*	*182*	*157*	*116*	*144*
Sl b	***0.38***	***0.38***	***0.33***	*0.30*	*0.21*	*0.21*	*0.16*	*0.08*	*0.11*	*0.11*
$\overline{m}$	*1.61*	***-0.19***	*5.21*	*1.07*	*3.93*	***0.15***	*1.62*	*1.82*	*0.71*	***0.33***
Sl a	***0.31***	***0.39***	*0.30*	*0.24*	***0.34***	*0.27*	*0.22*	*0.20*	*0.19*	*0.21*
S_a	***1.14***	*0.99*	***1.68***	*0.92*	***1.12***	*0.56*	*0.66*	*0.49*	*0.40*	*0.34*
μ_Δ	***10.0***	***6.48***	***5.12***	*4.95*	*3.85*	*3.03*	*2.68*	*2.51*	*1.97*	*1.66*

For f_0 = 1.0 Hz and R =3.0

Quake	*147*	*123*	*192*	*177*	*179*	*187*	*182*	*157*	*144*	*116*
Sl b	***0.32***	***0.30***	***0.35***	*0.29*	*0.27*	*0.23*	*0.21*	*0.21*	*0.16*	*0.15*
$\overline{m}$	*4.39*	***0.44***	***1.24***	*4.18*	*6.28*	*2.06*	***1.29***	*4.03*	*5.41*	*2.85*
Sl a	***0.39***	*0.30*	***0.34***	***0.31***	*0.27*	*0.24*	*0.22*	*0.20*	*0.21*	*0.19*
S_a	***2.46***	*1.45*	*1.91*	***2.21***	***2.66***	*1.47*	*1.25*	*1.85*	*1.94*	*1.30*
μ_Δ	***5.92***	***4.41***	***4.25***	*4.01*	*3.40*	*3.00*	*2.85*	*2.55*	*2.41*	*2.21*

For f_0 = 1.25 Hz and R =5.0

Quake	147	123	177	192	179	187	182	157	116	144
SI b	**0.36**	0.30	**0.31**	**0.33**	0.29	0.23	0.21	0.22	0.17	0.21
$\overline{m}$	5.51	**0.47**	3.89	2.75	**1.47**	**0.44**	3.66	2.60	3.84	6.91
SI a	**0.39**	0.30	**0.31**	**0.34**	0.27	0.24	0.22	0.20	0.19	0.21
S_a	**3.79**	1.58	**2.95**	2.62	2.05	1.32	2.31	2.06	2.22	**3.60**
μ_Δ	**11.77**	**9.03**	**8.49**	7.42	6.25	5.87	4.97	4.65	4.46	4.23

For f_0 = 2.0 Hz and R =4.0

Quake	147	177	144	192	123	179	187	116	182	157
SI b	**0.44**	**0.37**	**0.35**	0.32	0.23	0.30	0.23	0.25	0.25	0.24
$\overline{m}$	2.40	3.65	**-0.12**	4.11	2.22	**1.12**	2.93	4.09	2.80	**2.11**
SI a	**0.39**	**0.31**	0.21	**0.34**	0.30	0.27	0.24	0.19	0.22	0.20
S_a	**4.89**	**5.01**	2.83	**4.82**	3.15	3.05	3.41	4.22	3.54	3.07
μ_Δ	**11.09**	**8.52**	**6.40**	6.15	4.49	4.01	3.90	3.71	3.65	3.42

By confronting the ranking of the time histories based on the non-linear response to the one based on a given earthquake characteristic, it is possible to draw the following statements:

- The newly defined spectral intensity **SI b** always gives the best results.
- The very simple spectral acceleration characteristic **S_a** is not so bad – it figures out about 2 of the 3 worst cases. This performance is however largely tributary to the fact that large acceleration peaks occur in a set of recorded time histories.
- The average slope **$\overline{m}$** characteristic is mostly efficient for small strength reduction factors and low frequencies since the integration interval remains small and the influence of local peaks in the spectrum is fully taken into consideration.

The authors think that it is not really the ability of a characteristic to exactly predict the same rankings as the non-linear response that matters, but rather the assurance that the three worst time histories are detected. This is a specific feature of dynamic non-linear computations, which need to be carried out for at least three different time histories.

A.9 Comparison of ductility demand with and without fling

A.9.1 Recording Tcu048 (e: east component, n: north component)

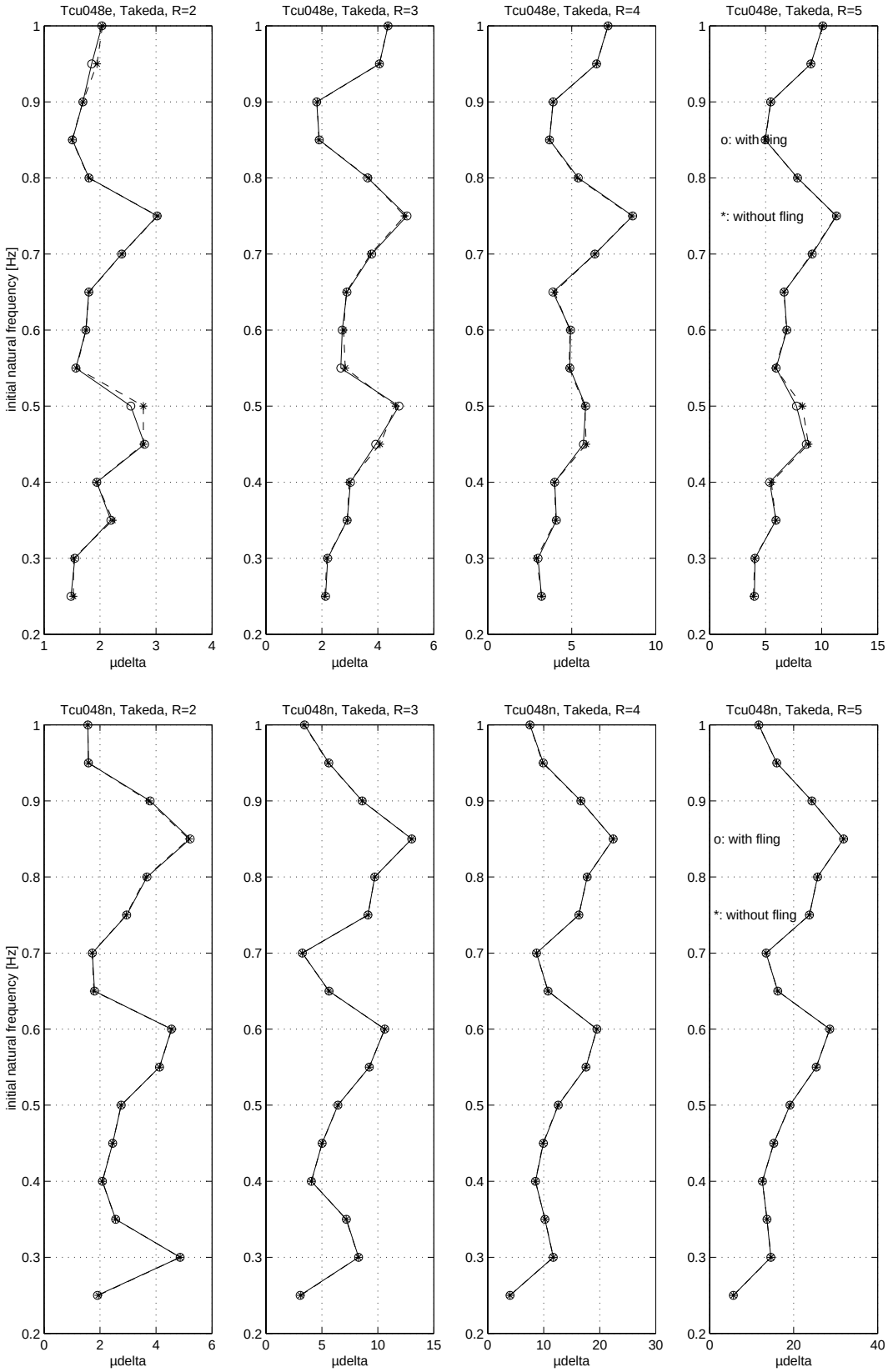

A.9.2 Recording Tcu049 (e: east component, n: north component)

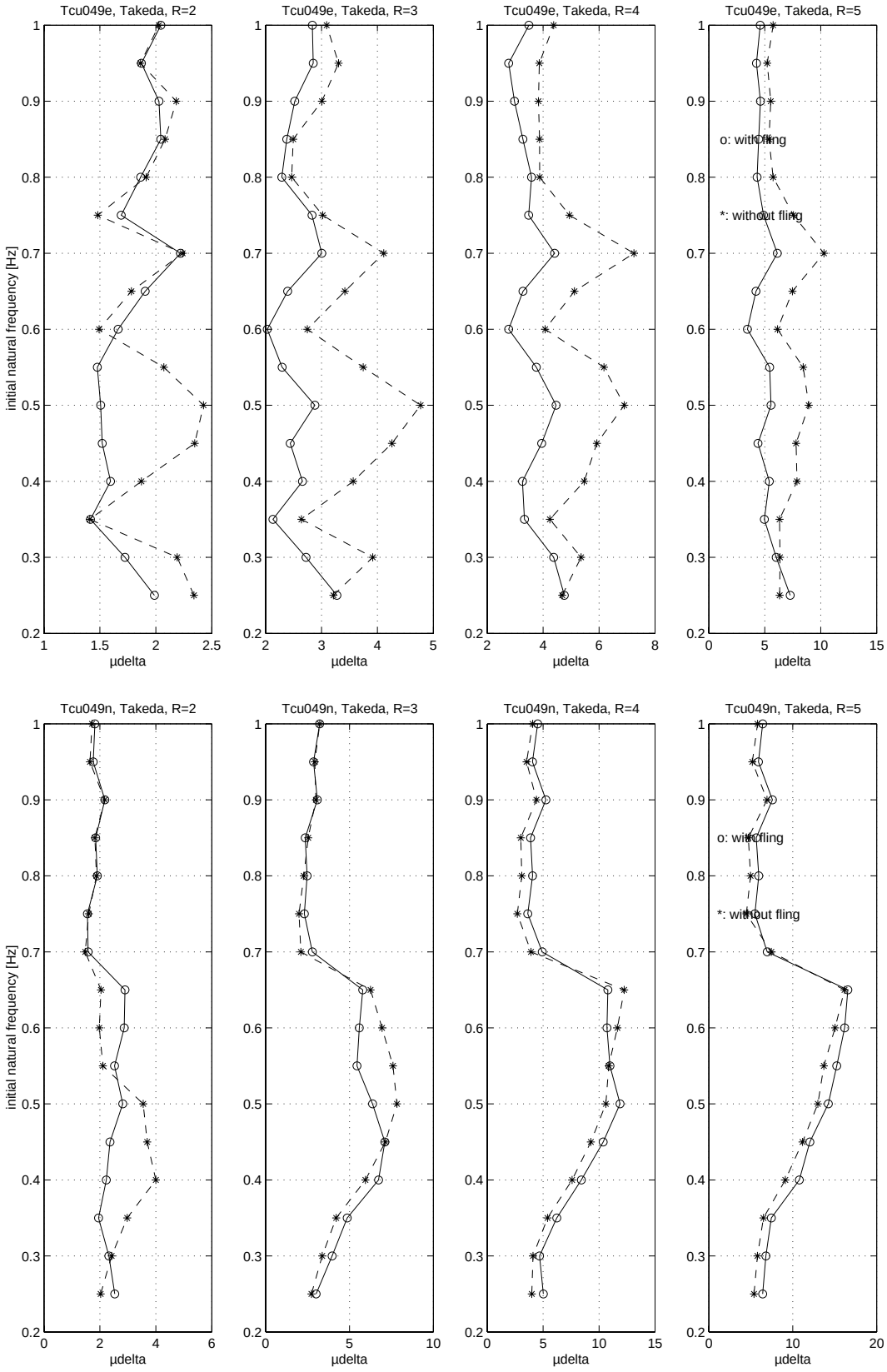

A.9.3 Recording Tcu050 (e: east component, n: north component)

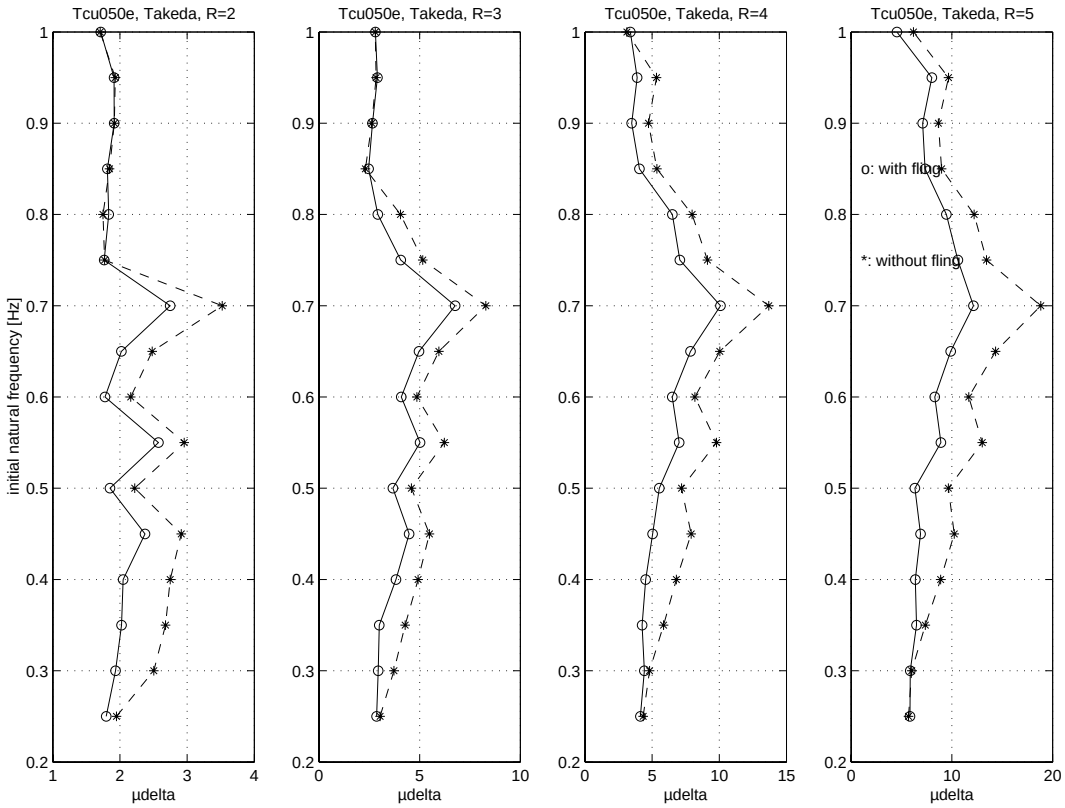

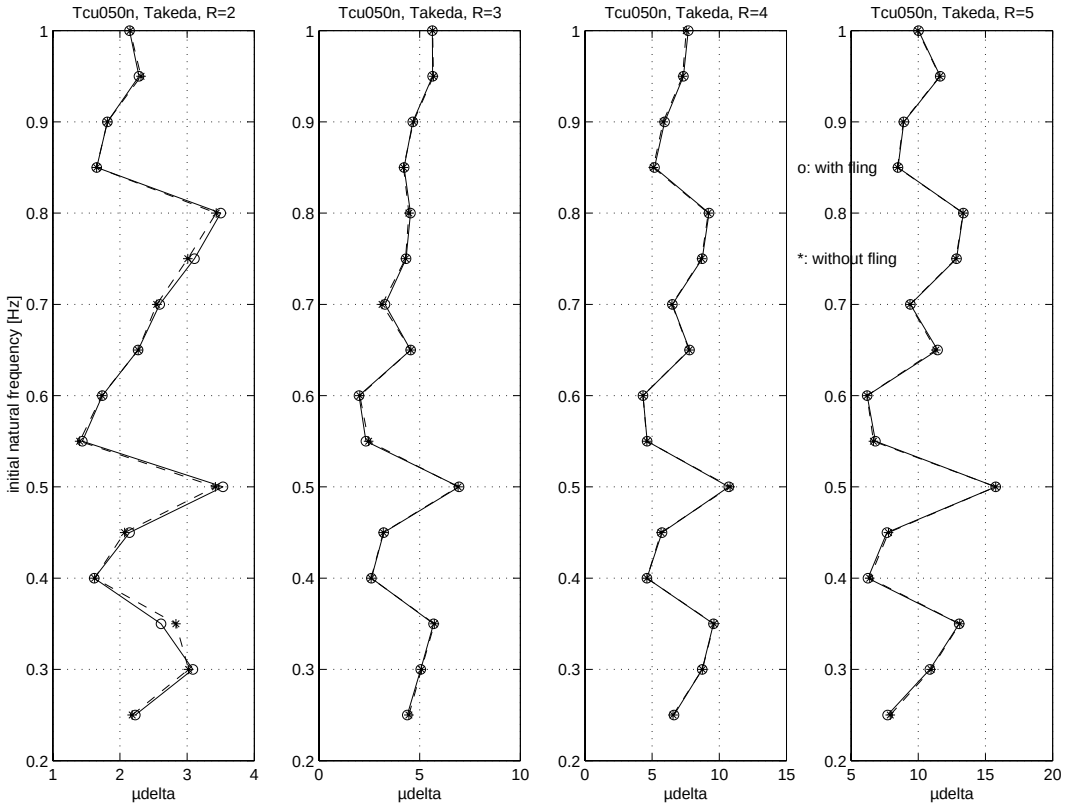

A.9.4 Recording Tcu051 (e: east component, n: north component)

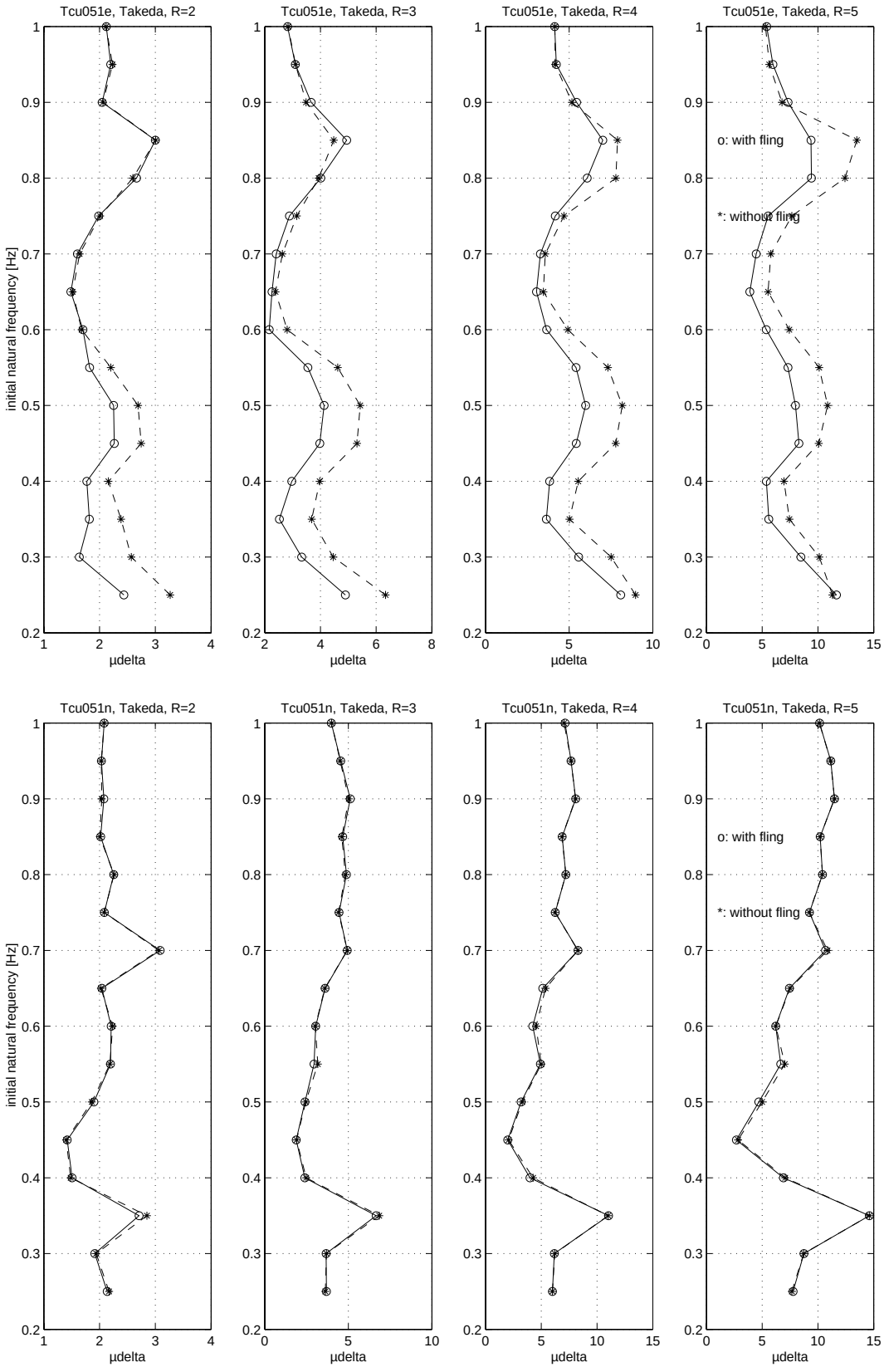

A.9.5 Recording Tcu053 (e: east component, n: north component)

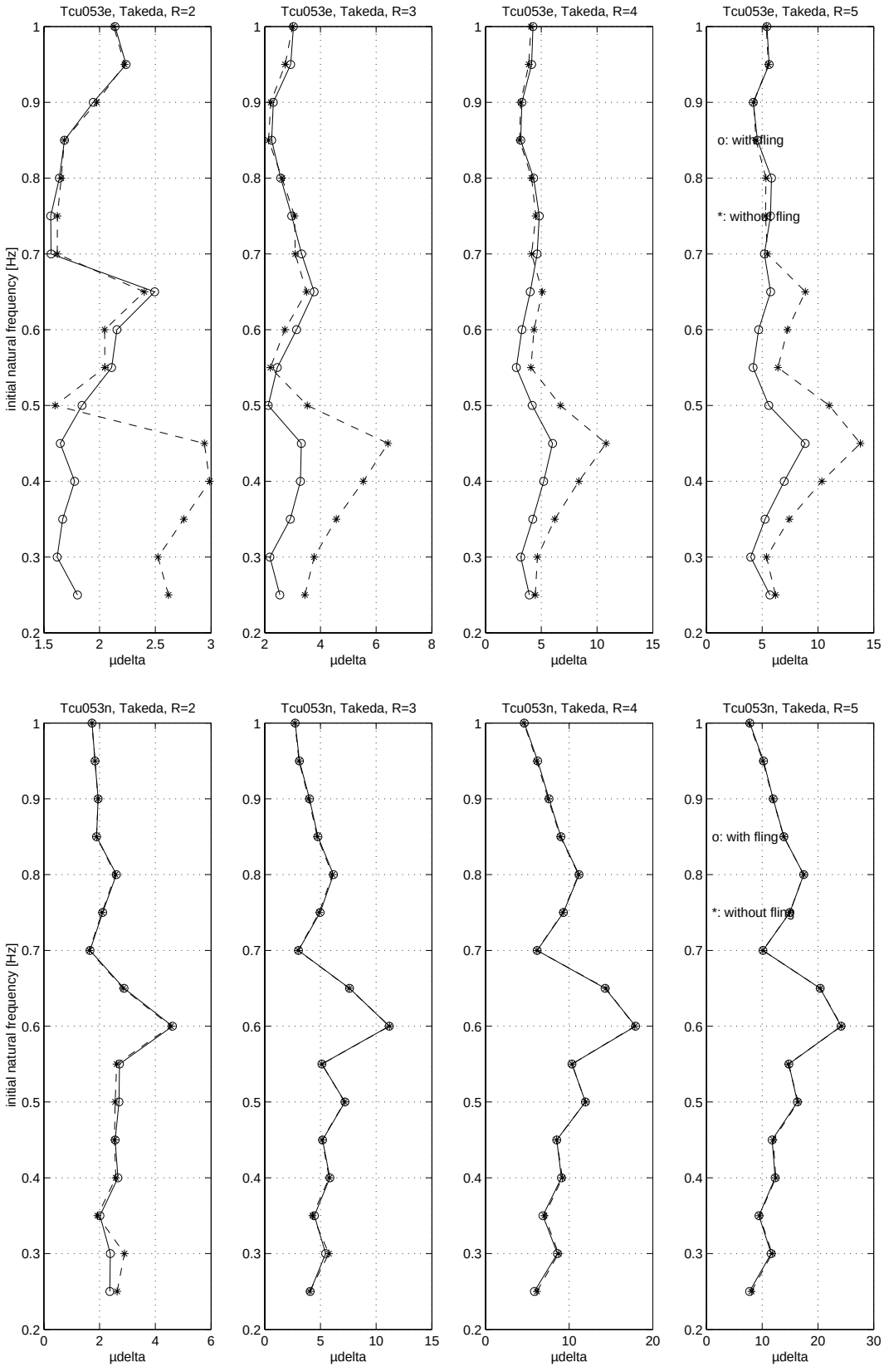

A.9.6 Recording Tcu054 (e: east component, n: north component)

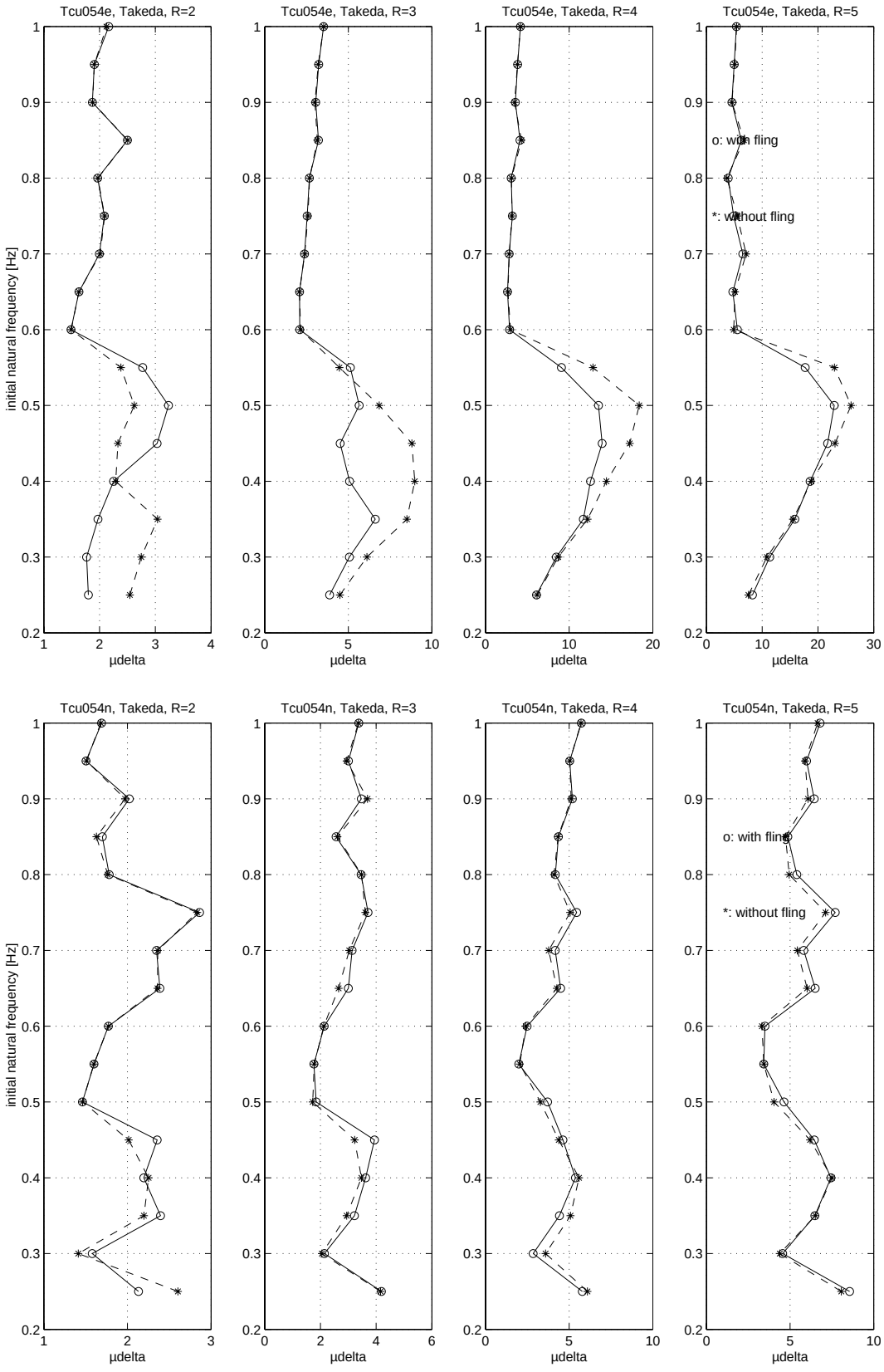

A.9.7 Recording Tcu055 (e: east component, n: north component)

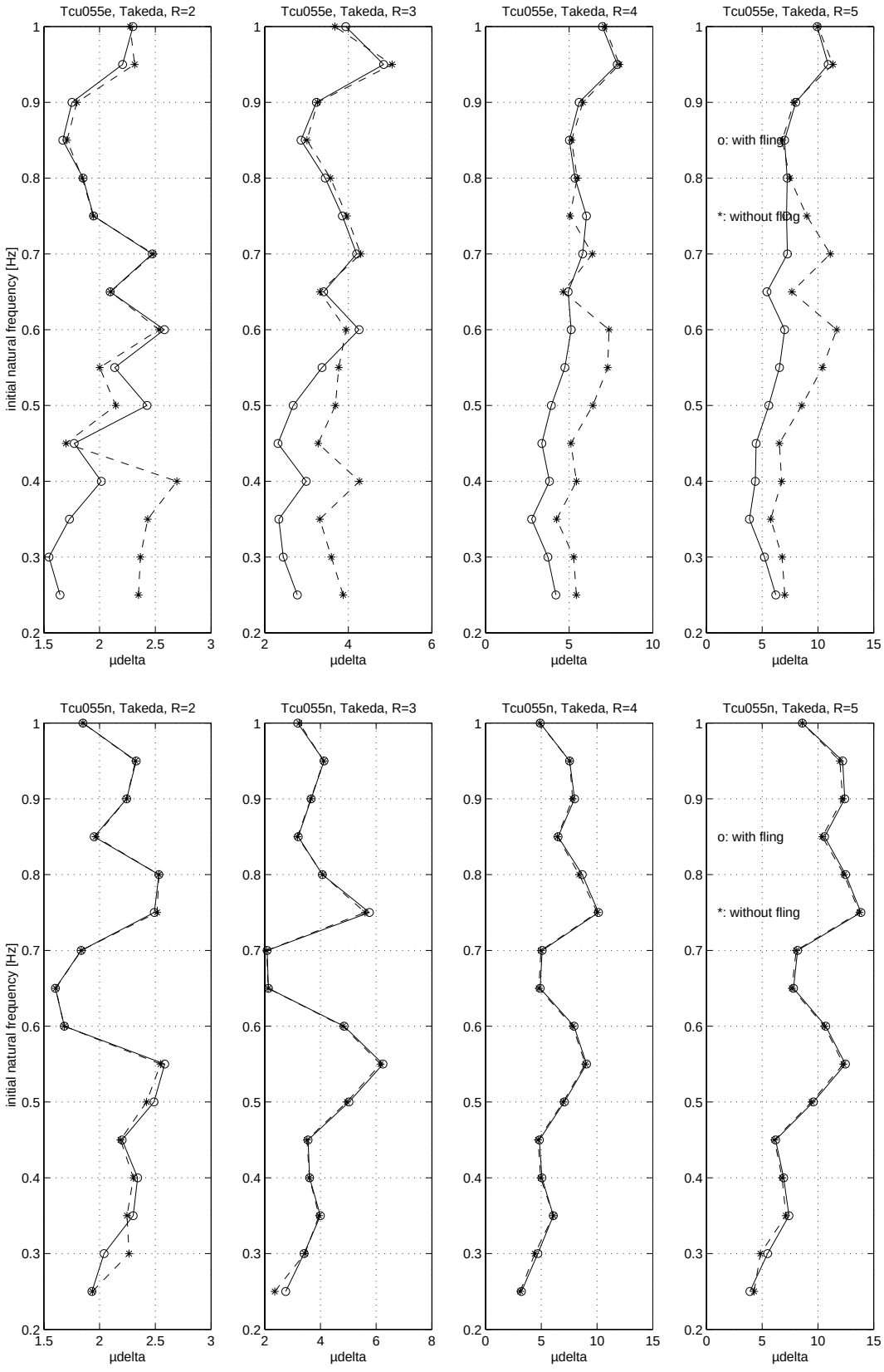

A.9.8 Recording Tcu056 (e: east component, n: north component)

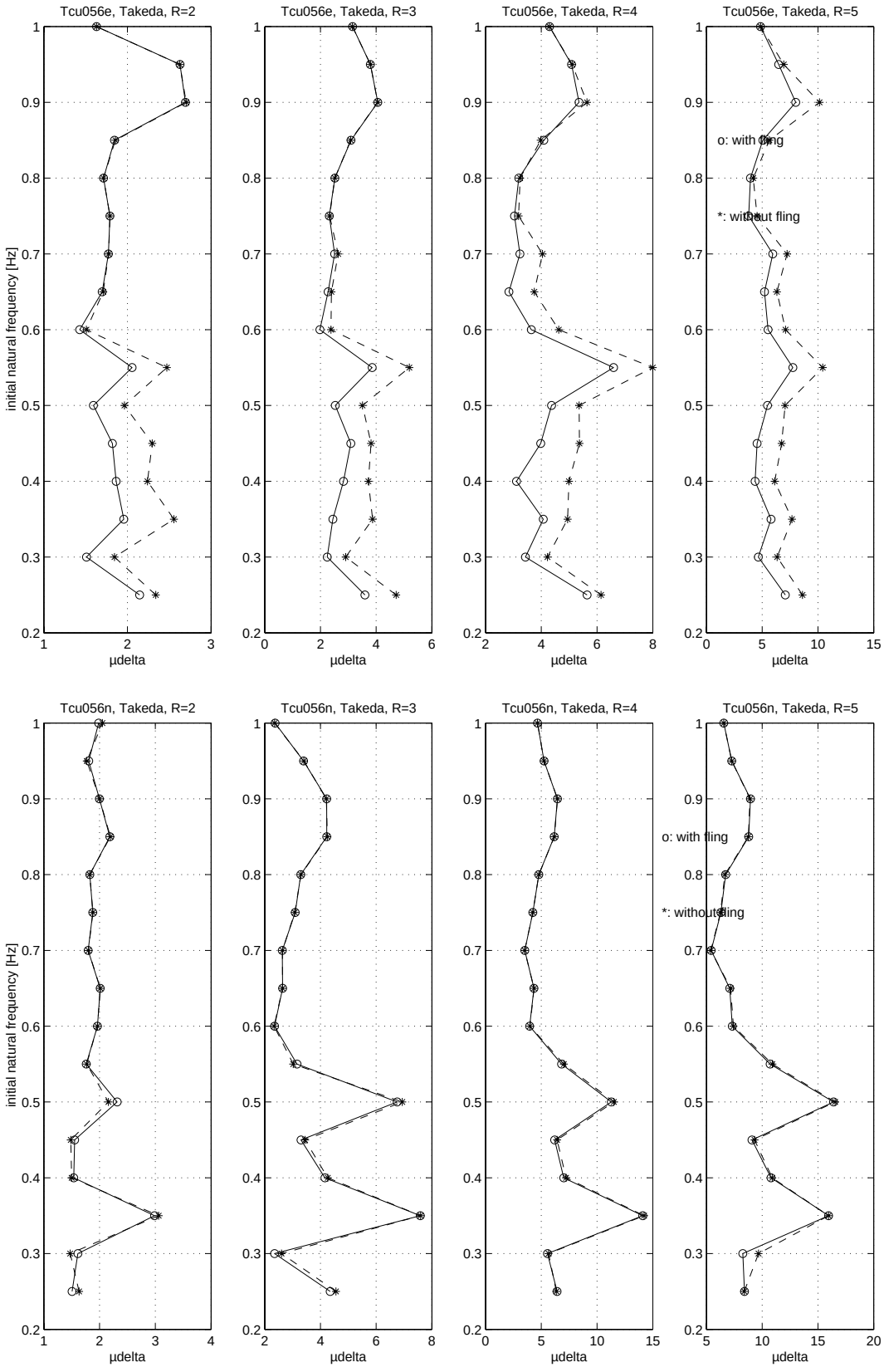

A.9.9 Recording Tcu057 (e: east component, n: north component)